1994-09

The ambiguity function of the stepped frequency radar

Huang, Jen-Chih

Monterey, California. Naval Postgraduate School

NAVAL POSTGRADUATE SCHOOL

Monterey, California

THESIS

THE AMBIGUITY FUNCTION OF THE STEPPED FREQUENCY RADAR

by

Huang, Jen-Chih

September 1994

Thesis Advisor: Gurnam S. Gill

Approved for public release; distribution is unlimited.

REPORT DOCUMENTATION PAGE

Form Approved OMB No. 0704

1. AGENCY USE ONLY *(Leave blank)*	2. REPORT DATE	3. REPORT TYPE AND DATES COVERED
	September, 1994	Master's Thesis, Final

4. TITLE AND SUBTITLE
THE AMBIGUITY FUNCTION OF THE STEPPED FREQUENCY RADAR.

5. FUNDING NUMBERS

6. AUTHOR(S)
Jen-Chih Huang

7. PERFORMING ORGANIZATION NAME(S) AND ADDRESS(ES)
Naval Postgraduate School
Monterey CA 93943-5000

8. PERFORMING ORGANIZATION REPORT NUMBER

9. SPONSORING/MONITORING AGENCY NAME(S) AND ADDRESS(ES)

10. SPONSORING/MONITORING AGENCY REPORT NUMBER

11. SUPPLEMENTARY NOTES The views expressed in this thesis are those of the author and do not reflect the official policy or position of the Department of Defense or the U.S. Government.

12a. DISTRIBUTION/AVAILABILITY STATEMENT Approved for public release; distribution unlimited

12b. DISTRIBUTION CODE
A

13. ABSTRACT *(maximum 200 words)*

High range resolution radar sytems have many advantages such as target classification, resolution of multiple target, accurate range profile and detection of low radar cross section (RCS) targets in clutter. High range resolution requires large bandwidths. Stepped frequency waveforms can achieve high range resolution by increasing the effective bandwidth without increasing the instantaneous bandwidth which would increase the hardware requirements including higher analog to digital (A/D) sampling rates which are limited by existing technology. Under today's hardware limitations, the stepped frequency waveform becomes very important. This thesis briefly discusses the stepped frequency radar and associated signal processing, it investigates the ambiguity function of the stepped frequency waveform and the stepped frequency radar system. Mathematical expressions of ambiguity functions are derived and the improvement of clutter suppression capability for the stepped frequency radar by rejecting initial pulses is also discussed.

14. SUBJECT TERMS	15. NUMBER OF PAGES
Stepped frequency waveform, Auto-ambiguity Function, Cross-ambiguity Function	99
	16. PRICE CODE

17. SECURITY CLASSIFICATION OF REPORT	18. SECURITY CLASSIFICATION OF THIS PAGE	19. SECURITY CLASSIFICATION OF ABSTRACT	20. LIMITATION OF ABSTRACT
Unclassified	Unclassified	Unclassified	UL

NSN 7540-01-280-5500

Standard Form 298 (Rev. 2-89)
Prescribed by ANSI Std. 239-18

Approved for public release; distribution is unlimited.

THE AMBIGUITY FUNCTION OF THE STEPPED FREQUENCY RADAR

Huang, Jen-Chih
Major, Taiwan Army
B.S, Chung Cheng Institute of Technology, 1984

Submitted in partial fulfillment
of the requirements for the degree of

MASTER OF SCIENCE IN ELECTRICAL ENGINEERING
and
MASTER OF SCIENCE IN SYSTEMS ENGINEERING

from the

NAVAL POSTGRADUATE SCHOOL
September 1994

Author: [redacted]
Huang, Jen-Chih

Approved By: [redacted]
Gurnam S. Gill, Thesis Advisor

[redacted]
Tri T. Ha, Second Reader

[redacted]
Michael A. Morgan, Chairman
Department of Electrical and Computer Engineering

[redacted]
Frederic H. Levien, Chairman
Department of Electronic Warfare

ABSTRACT

High range resolution radar systems have many advantages such as target classification, resolution of multiple targets, accurate range measurement, target range profile and detection of low radar cross section (RCS) targets in clutter. High range resolution requires large bandwidths. Stepped frequency waveforms can achieve high range resolution by increasing the effective bandwidth without increasing the instantaneous bandwidth which would increase the hardware requirements including higher analog to digital (A/D) sampling rates which are limited by existing technology. Under today's hardware limitations, the stepped frequency waveform becomes very important. This thesis briefly discusses the stepped frequency radar and associated signal processing, it investigates the ambiguity function of the stepped frequency waveform and the stepped frequency radar system. Mathematical expressions of ambiguity functions are derived and the improvement of clutter suppression capability for the stepped frequency radar by rejecting initial pulses is also discussed.

TABLE OF CONTENTS

LIST OF FIGURES

I. INTRODUCTION

High range resolution radar systems have many advantages such as target classification, resolution of multiple targets, accurate range measurement, target range profile and detection of low radar cross section (RCS) targets in clutter. High range resolution is typically achieved either by decreasing the duration of the transmitted signal or by modulating a transmitted signal of relatively longer duration. In either case, the instantaneous bandwidth of the signal goes up and thereby increases the hardware requirements to include higher A/D sampling rates (which are limited by existing technology). However, with the stepped frequency waveform, it is possible to achieve higher range resolutions with lower instantaneous bandwidths and lower A/D sampling rates. Irrespective of the waveform or compression method used, high range resolution requires large bandwidths. For the stepped frequency waveform, a large bandwidth is obtained sequentially by changing the carrier frequency in steps over several pulses instead of within a single pulse. This waveform potentially can be implemented in high performance radar systems with lower A/D sampling rates, which is one of the current bottlenecks in the development of radar systems. Because of the importance of the stepped frequency waveform, this thesis briefly discusses the stepped frequency radar, its associated signal processing, and analyzes it by the ambiguity function. In Chapter II the stepped frequency waveform and its corresponding radar system are introduced. In

Chapter III the matched filter and the correlation definition of the ambiguity function are first discussed. The properties and applications of the ambiguity function are also briefly discussed. The mathematical expression of the auto-ambiguity function for the stepped frequency waveform is then derived from the definition and is verified by comparing the ambiguity diagram with one obtained by simulation. Finally, the mathematical expression of the cross-ambiguity function for the stepped frequency radar signal processor is derived and verified, and the improvement of the clutter suppression capability for the stepped frequency radar by the rejection of initial pulses is discussed. In Appendix A, the ambiguity functions for the single pulse, constant frequency pulse train, linear frequency modulated (LFM) pulse, and the discrete frequency modulated pulse are given for the purpose of comparison. Mathematical expressions of the ambiguity functions for these waveforms are derived and verified. In Appendix B, the computer programs of ambiguity functions for all the waveforms discussed in the thesis are listed.

II. OPERATING PRINCIPLES OF THE STEPPED FREQUENCY RADAR

A. STEPPED FREQUENCY WAVEFORM

The stepped frequency waveform can be described by a series of N coherent pulses, where the carrier frequency increases from pulse to pulse by a fixed increment Δf as shown in Figure 1. Each pulse has a fixed pulse width T_s, and the pulses are transmitted at a fixed pulse repetition interval (PRI). The frequency of the kth pulse is given by

$$f_k=f_0+(k-1)\Delta f, \tag{1}$$

where f_0 is the nominal carrier frequency and Δf is the frequency step size. [Ref. 1, pp. 160-161]

The instantaneous bandwidth of this waveform is approximately equal to the inverse of the pulse width and is much less than the effective bandwidth. The waveform's effective bandwidth, denoted as B_{eff}, is determined by the product of the number of pulses N, and the frequency step size Δf as given below.

$$B_{eff}=N\Delta f \tag{2}$$

The range resolution for any waveform is dependent on the effective bandwidth of the waveform. The range resolution of the stepped frequency waveform is given as

$$\Delta r = \frac{c}{2N\Delta f} \tag{3}$$

where c is the speed of the light. Thus the range resolution can be made finer by increasing the effective bandwidth $N\Delta f$. [Ref. 2, p. 234]

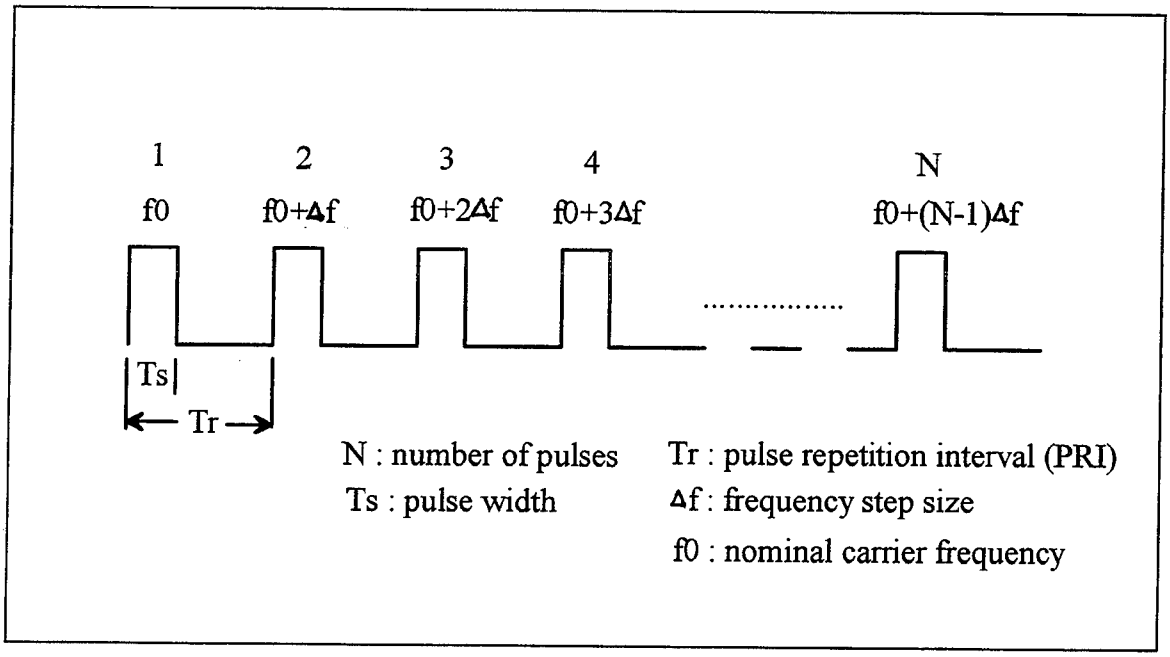

Figure 1. The Stepped Frequency Waveform

The effective bandwidth is achieved by the signal processing of the data obtained during the coherent processing interval (CPI), which usually is the time on target. The CPI is given by the product of the number of pulses N and the pulse repetition interval (PRI).

$$CPI=N\times PRI \tag{4}$$

B. SYSTEM DESCRIPTION

The block diagram of a radar which employs a stepped frequency waveform is shown in Figure 2. The transmitted signal in this radar is generated as in conventional coherent radars by mixing RF frequency (STALO) and IF frequency (COHO). However, the frequency step in each pulse is added by the frequency synthesizer as shown in Figure 2. On the receiver side, a reverse operation of taking out the RF, step, and IF frequencies is performed. The IF amplifier serves as a matched filter to the envelope of each individual pulse. The output of the synchronous detector is a video signal in the form of in-phase and quadrature (I-Q) components. The output of the A/D is stored and organized according to range bins. Received signals from all N pulses in each range bin is collected. This data may be weighted before taking the DFT. The output of the DFT represents a finely resolved range bin. The size of the original range bin is $c\tau/2$. However, after DFT, the width of the subdivision of a finely resolved range bin is $c\tau/2N\Delta f\tau$, which is equivalent to having a bandwidth of $N\Delta f$ [Ref.2, p. 236]. The unambiguous range R_u for this waveform is $c/2\Delta f$. This will be quite short but it may not be a problem as it is applicable within the same range bin. For avoiding wrap around the target, R_u should be greater than the target extent.

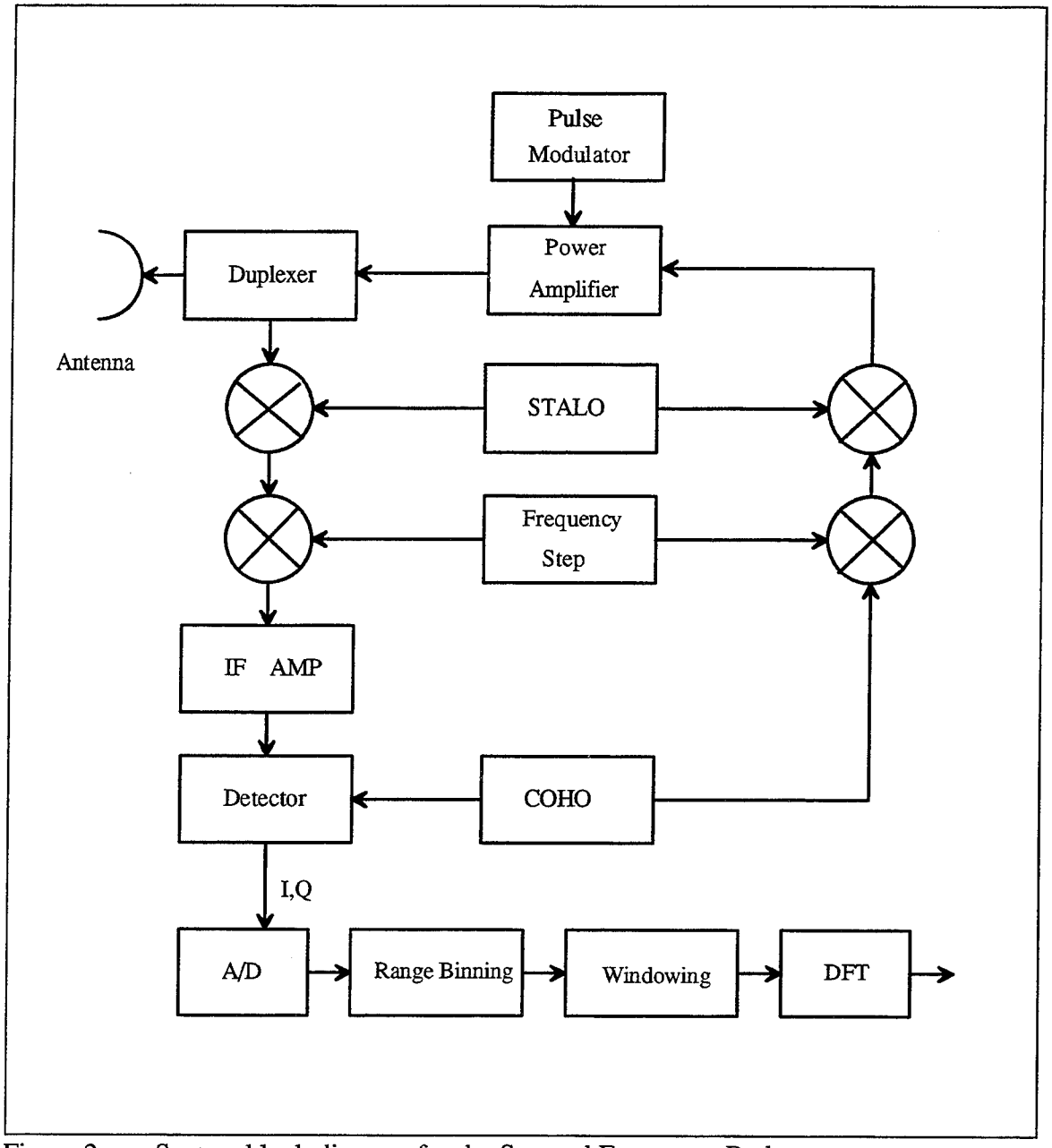

Figure 2. System block diagram for the Stepped Frequency Radar

III. ANALYSIS OF THE STEPPED FREQUENCY RADAR BY THE AMBIGUITY FUNCTION

A. INTRODUCTION TO AMBIGUITY FUNCTION

1. Matched Filter

The matched filter maximizes the output peak signal to noise power ratio for the detection of a known signal. In the presence of additive white Gaussian noise, the impulse response of the matched filter is the complex conjugate of the image of the received waveform, $h(t)=s^*(t_1-t)$, where s(t) is the received signal, that is, it is the same as the received signal run backward in time starting from fixed time t_1. [Ref. 3, p. 261] In order to simplify the mathematical developement, it is customary to set t_1 at zero. The output of the matched filter is then written as

$$y(t)=\int_{-\infty}^{\infty} s(\lambda)h(t-\lambda)d\lambda=\int_{-\infty}^{\infty} s(\lambda)s^*(\lambda-t)d\lambda \tag{5}$$

2. Definition of the Ambiguity Function

If the transmitted signal $S_t(t)$ is $u(t)e^{j2\pi f_0 t}$, then received signal $S_r(t)$ is given by $u(t-T_D)e^{j2\pi(f_0+f_d)(t-T_D)}$, where T_D is the unknown round trip time delay given by $\frac{2R}{c}$ and f_d is the Doppler shift of the returned signal. Assuming that the radar receiver is matched to the transmitted signal, we obtain the output of the matched filter as

$$S_o\left(T_D^{'}\right)=\int_{-\infty}^{\infty} u(t-T_D)e^{j2\pi(f_0+f_d)(t-T_D)}\times u^*\left(t-T_D^{'}\right)e^{-j2\pi f_0\left(t-T_D^{'}\right)}dt\ , \tag{6}$$

where $T_D^{'}$ is the estimate of time delay.

It is customary to set $T_D^{'}$ and f_0 equal to zero, and to define $T_D - T_D^{'}$ as τ. The output of the matched filter is then

$$S_0(\tau) = e^{-j2\pi f_d \tau} \times \int_{-\infty}^{\infty} u(t-\tau)u^*(t)e^{j2\pi f_d t}dt. \tag{7}$$

Since the interest is only in the magnitude of the matched filter output, neglecting the first exponential term, we obtain the output of the matched filter as

$$X(\tau, f_d) = \int_{-\infty}^{\infty} u(t-\tau)u^*(t)e^{j2\pi f_d t}dt \tag{8}$$

In this form a positive τ indicates a target beyond the reference delay t_0, and a positive f_d indicates an incoming target [Ref. 4]. In the literature the term "Ambiguity Function" is interchangeably used for $X(\tau,f_d)$, $|X(\tau,f_d)|$, and $|X(\tau,f_d)|^2$. In this thesis, the plot of $|X(\tau,f_d)|^2$ is called the ambiguity diagram. If the receiver filter is matched to the transmitted signal, $|X(\tau,f_d)|^2$ is termed the auto-ambiguity function, otherwise, it is termed the cross-ambiguity function.

3. Properties of the Ambiguity Function

The function $|X(\tau,f_d)|^2$ has the following properties [Ref. 5, p. 412]:

Maximum value of $|X(\tau,f_d)|^2 = |X(0,0)|^2 = (2E)^2$, (9)

$$|X(-\tau,-f_d)|^2 = |X(\tau,f_d)|^2, \tag{10}$$

$$|X(\tau,0)|^2 = |\int_{-\infty}^{\infty} u(t-\tau)u^*(t)dt|^2, \tag{11}$$

$$|X(0,f_d)|^2 = |\int_{-\infty}^{\infty} u^2(t)e^{j2\pi f_d}dt|^2, \tag{12}$$

$$\int_{-\infty}^{\infty}\int_{-\infty}^{\infty} |X(\tau,f_d)|^2 d\tau df_d = (2E)^2 . \qquad (13)$$

The first equation given above, Equation 9, states that the maximum value of the ambiguity function occurs at the origin and its value is $(2E)^2$, where E is the energy contained in the echo signal. Equation 10 shows that the ambiguity function is symmetric about the origin. Equation 11 describes that the ambiguity function along the time delay axis is the auto-correlation function of the complex envelope of the transmitted signal. Equation 12 shows that along the frequency shift axis the ambiguity function is proportional to the spectrum of $u^2(t)$. Equation 13 states that the total volume under the ambiguity function is a constant equal to $(2E)^2$.

The ideal ambiguity diagram consists of a single peak of infinitesimal thickness at the origin and is zero everywhere else, as shown in Figure 3. The single spike eliminates any ambiguities, and its infinitesimal thickness at the origin permits the frequency and the echo delay time to be determined simultaneously to as high a degree of accuracy as desired. It also permits the resolution of two targets no matter how close together they are on the ambiguity diagram. Because of two restrictions the ideal ambiguity function is not possible; first, the maximum height of the ambiguity function must be equal to $(2E)^2$, which is limited, and second, the total area under the ambiguity function must be finite and equal to $(2E)^2$. A reasonable approximation to the ideal ambiguity function might appear as shown in Figure 4. This waveform does not result in ambiguity since there is only one peak, but the single peak might be too broad to satisfy the requirements of accuracy and resolution. If the peak is made too narrow, the requirement for a constant

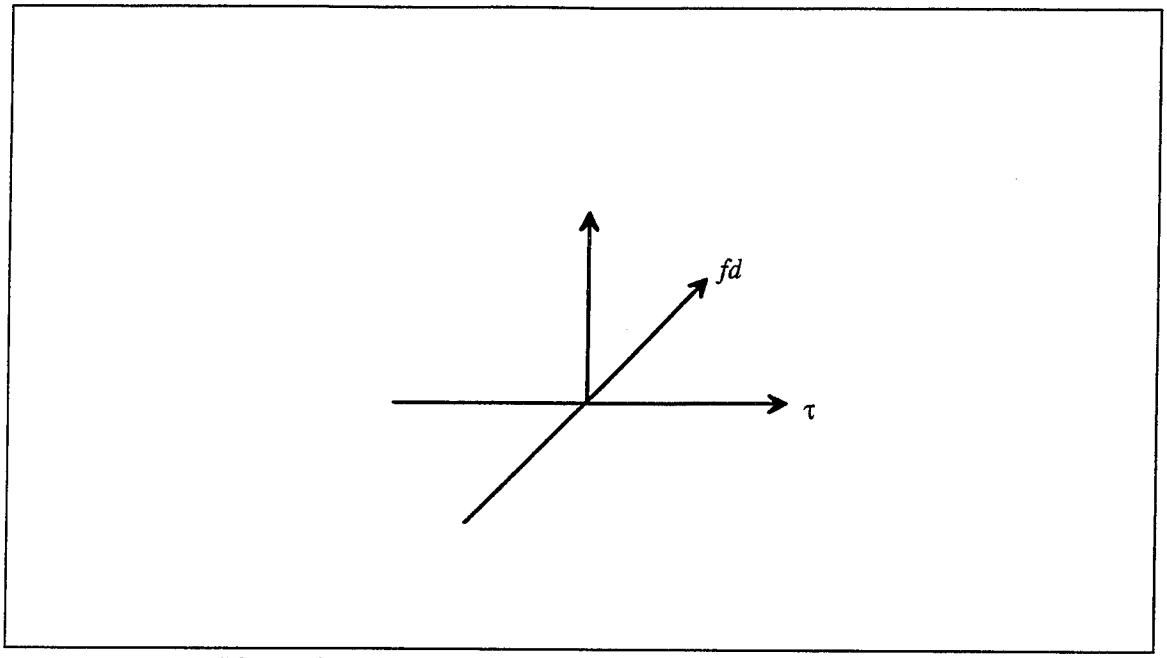

Figure 3. Ideal ambiguity diagram "after Ref. [5]."

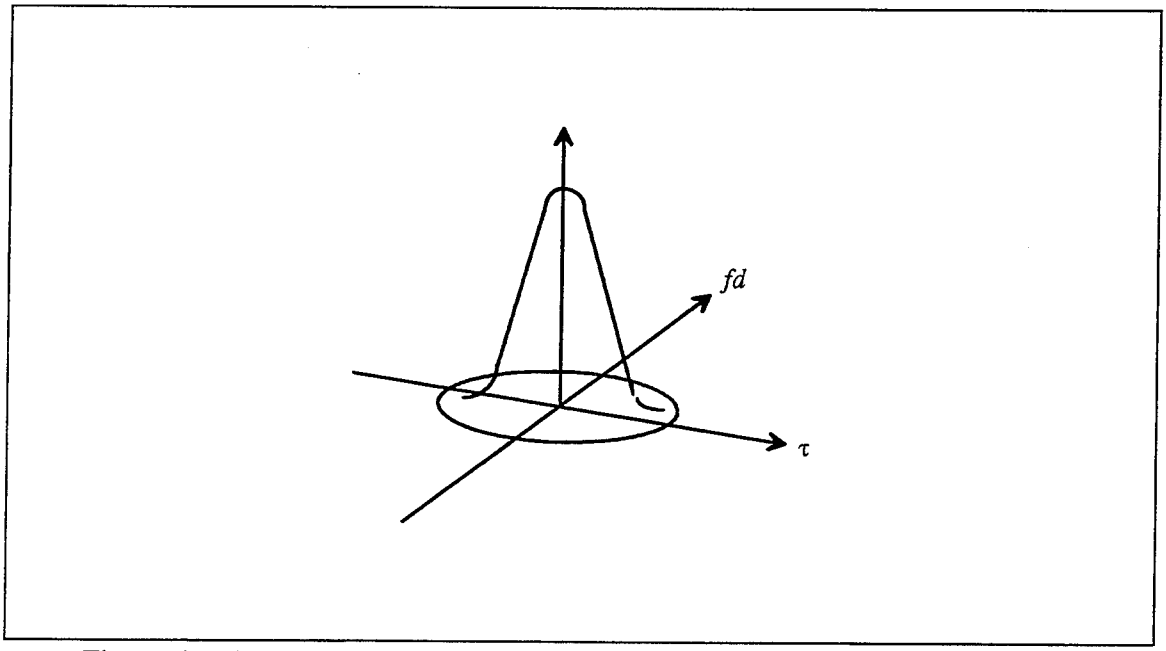

Figure 4. The approximation to the ideal ambiguity diagram "after Ref. [5]."

volume might cause peaks to form at regions of the ambiguity diagram other than the origin and give rise to ambiguities. Thus the requirements for accuracy and ambiguity may not always be simultaneously possible to satisfy. [Ref. 5, pp. 412-413]

The particular waveform transmitted by a radar is chosen to satisfy the requirements for (1) detection, (2) measurement accuracy, (3) resolution, (4) ambiguity, and (5) clutter rejection. The ambiguity diagram may be used to assess qualitatively how well a waveform can achieve these requirements. The maximum value of the ambiguity function is an indication of the radar's detection capabilities. Since the ambiguity diagram is often normalized so that the maximum value is equal to one, the ambiguity diagram is seldom used to assess the detection capabilities of the waveform. The accuracy with which the range and the velocity can be measured by a particular waveform depends on the width of the spike, centered at $|X(0,0)|^2$, along the time and frequency axes. The resolution is also related to the width of the central spike, but in order to resolve two closely located targets the central spike must be isolated. It cannot have any high peaks nearby that might mask another target close to the desired target. A waveform that yields good resolution will also yield good accuracy, but the reverse is not always true. The presence of additional spikes can lead to ambiguity in the measurement of target parameters. An ambiguity measurement is one in which there is more than one choice available for the correct value of a parameter, but only one choice is appropriate. Thus the correct value is uncertain. The ambiguity diagram may be used to determine the ability of a waveform to reject clutter. If the transmitted waveform is to have good clutter-rejection

properties, the ambiguity diagram should have little or no response in the regions of clutter [Ref. 5, pp. 418-420]. Some examples of the ambiguity function are shown in Appendix A which includes single pulse, pulse train, linear frequency modulation pulse, and stepped frequency modulation pulse.

B. DERIVATION OF THE AUTO-AMBIGUITY FUNCTION FOR THE STEPPED FREQUENCY RADAR

In order to derive the auto-ambiguity function, according to the definition, Equation 8, we need the expression of the complex envelope of the transmitted signal. The transmitted signal of the stepped frequency radar consisting of a train of N pulses and changing carrier frequency from pulse to pulse by fixed increment Δf is shown in Figure 1. It is mathematically represented as

$$S_t(t) = a_t \sum_{n=0}^{N-1} u(t - nT_r) e^{j2\pi(f_0 + n\Delta f)t}, \tag{14}$$

where
$$u(t - nT_r) = \begin{cases} 1, & \text{if } nT_r \le t \le nT_r + T_s, \\ 0, & \text{elsewhere,} \end{cases} \tag{15}$$

$f_{step} = n\Delta f$, $n = 0, ..., N-1$,and

$f_0 = f_{coho} + f_{stalo}$,

f_{coho} : the frequency of the stable coherent oscillator ,

f_{stalo} : the frequency of the stable local oscillator ,

f_{step} : step frequency,

Δf : the frequency step size,

N : the number of the pulse sequences,

T_r : pulse repetition interval (PRI),

T_s : pulse width,

a_t : the amplitude of the transmitted signal.

The transmitted signal can be rewritten as

$$S_t(t) = a_t\left[\sum_{n=0}^{N-1} u(t-nT_r)e^{j2\pi n\Delta ft}\right]e^{j2\pi f_0 t}$$

$$= a_t U(t)e^{j2\pi f_0 t} \tag{16}$$

where $U(t) = \sum_{n=0}^{N-1} u(t-nT_r)e^{j2\pi n\Delta ft}$ is the complex envelope of the pulse sequence. The signal received due to a discrete scatterer can be written as

$$S_r(t) = a_r U(t-\tau)e^{j2\pi(f_0+f_d)(t-\tau)} \tag{17}$$

where

a_r : the amplitude constant,
τ : the round trip time between the radar and the scatterer,
f_d : the Doppler frequency shift due to the normal relative velocity between the radar and the scatterer,

$$\tau = \frac{2R}{c}, \tag{18}$$

and

$$f_d = \frac{2v_r}{c}f_0. \tag{19}$$

Substituting the complex envelope, U(t) , of the transmitted signal into Equation 8, we obtain the auto-ambiguity function of the stepped frequency radar as

$$X(\tau,f_d) = \int_{-\infty}^{\infty}\sum_{m=0}^{N-1} u(t-mT_r-\tau)e^{j2\pi m\Delta f(t-\tau)}\times\sum_{n=0}^{N-1} u^*(t-nT_r)e^{-j2\pi n\Delta ft}\times e^{j2\pi f_d t}dt. \tag{20}$$

Changing variable t-nT$_r$ by t', we change the above equation to

$$X(\tau,f_d) = \sum_{m=0}^{N-1}\sum_{n=0}^{N-1} e^{-j2\pi n^2\Delta fT_r}\times e^{j2\pi mn\Delta fT_r}\times e^{-j2\pi m\Delta f\tau}\times e^{j2\pi f_d nT_r}$$

$$\times\int_{-\infty}^{\infty} u^*\left(t'\right)u\left(t'-(m-n)-\tau\right)e^{j2\pi(m-n)\Delta ft'}e^{j2\pi f_d t'}dt'. \tag{21}$$

Defining the round trip time τ in terms of integer and fraction parts

$$\tau = (p+\gamma)T_r, \tag{22}$$

where p is an integer, γ is the fraction, and $0 \le \gamma < 1$, we obtain the ambiguity function as

$$X(\tau, f_d) = (T_s - \gamma T_r) \times e^{j\pi(f_d - p\Delta f)(T_s + \gamma T_r)} \times e^{j2\pi p \Delta f \tau} \times \frac{\sin \pi(f_d - p\Delta f)(T_s - \gamma T_r)}{\pi(f_d - p\Delta f)(T_s - \gamma T_r)}$$

$$\times \sum_{n=\max(0,p)}^{\min(N-1,N-1+p)} e^{j2\pi n(f_d - p\Delta f)T_r} \times e^{-j2\pi n \Delta f \tau},$$

$$\text{for } 0 \le \gamma < \frac{T_s}{T_r}, \tag{23-1}$$

$$= (T_s + (\gamma - 1)T_r) \times e^{j\pi(f_d - (p+1)\Delta f)(T_s + (\gamma-1)T_r)} \times \frac{\sin \pi(f_d - (p+1)\Delta f)(T_s + (\gamma-1)T_r)}{\pi(f_d - (p+1)\Delta f)(T_s + (\gamma-1)T_r)}$$

$$\times e^{j2\pi(p+1)\Delta f \tau} \times \sum_{n=\max(0,p+1)}^{\min(N-1,N+p)} e^{j2\pi n(f_d - (p+1)\Delta f)T_r} \times e^{-j2\pi n \Delta f \tau},$$

$$\text{for } 1 - \frac{T_s}{T_r} \le \gamma < 1, \text{ and} \tag{23-2}$$

$$= 0, \qquad \text{elsewhere.} \tag{23-3}$$

After simplifying the summation term and taking the absolute value, we obtain the expression for the auto-ambiguity function as

$$|X(\tau, f_d)| = (T_s - \gamma T_r) \times \left| \frac{\sin \pi(f_d - p\Delta f)(T_s - \gamma T_r)}{\pi(f_d - p\Delta f)(T_s - \gamma T_r)} \right| \times \left| \frac{\sin \pi(f_d - (2p+\gamma)\Delta f)(N - |p|)T_r}{\sin \pi(f_d - (2p+\gamma)\Delta f)T_r} \right|,$$

$$\text{for } 0 \le \gamma < \frac{T_s}{T_r}, \tag{24-1}$$

$$|X(\tau,f_d)| = (T_s+(\gamma-1)T_r)\times\left|\frac{\sin\pi(f_d-(p+1)\Delta f)(T_s+(\gamma-1)T_r)}{\pi(f_d-(p+1)\Delta f)(T_s+(\gamma-1)T_r)}\right|\times\left|\frac{\sin\pi(f_d-(2p+\gamma+1)\Delta f)(N-|p+1|)T_r}{\sin\pi(f_d-(2p+\gamma+1)\Delta f)T_r}\right|,$$

$$\text{for } 1-\frac{T_s}{T_r}\le\gamma<1, \tag{24-2}$$

$$=0, \qquad \text{elsewhere.} \tag{24-3}$$

The auto-ambiguity function along the Doppler frequency shift axis can be expressed as

$$|X(0,f_d)| = T_s\times\left|\frac{\sin\pi f_d T_s}{\pi f_d T_s}\right|\times\left|\frac{\sin\pi f_d N T_r}{\sin\pi f_d T_r}\right|. \tag{25}$$

The auto-ambiguity function along the time delay axis can be expressed as

$$|X(\tau,0)| = (T_s-\gamma T_r)\times\left|\frac{\sin\pi(-p\Delta f)(T_s-\gamma T_r)}{\pi(-p\Delta f)(T_s-\gamma T_r)}\right|\times\left|\frac{\sin\pi(-(2p+\gamma)\Delta f)(N-|p|)T_r}{\sin\pi(-(2p+\gamma)\Delta f)T_r}\right|,$$

$$\text{for } 0\le\gamma<\frac{T_s}{T_r}, \tag{26-1}$$

$$=(T_s+(\gamma-1)T_r)\times\left|\frac{\sin\pi(-(p+1)\Delta f)(T_s+(\gamma-1)T_r)}{\pi(-(p+1)\Delta f)(T_s+(\gamma-1)T_r)}\right|\times\left|\frac{\sin\pi(-(2p+\gamma+1)\Delta f)(N-|p+1|)T_r}{\sin\pi(-(2p+\gamma+1)\Delta f)T_r}\right|,$$

$$\text{for } 1-\frac{T_s}{T_r}\le\gamma<1, \text{ and} \tag{26-2}$$

$$=0, \qquad \text{elsewhere}. \tag{26-3}$$

One can easily show that the auto-ambiguity function of the stepped frequency radar will become the ambiguity function of the pulse radar (shown in Appendix A) by setting Δf to zero. The ambiguity diagram, that is the plot of $|X(\tau,f_d)|^2$ for the stepped frequency waveform for the following parameters: number of pulses N equals to 4,

duty-cycle equals 0.2, and frequency step size Δf equals 2PRF is plotted in Figure 5. This plot somewhat looks like the ambiguity function of the pulse train rotated at an angle. The contour plot of the ambiguity function is shown in Figure 6. Plots of a cut along the frequency axis for τ=0 and a cut along the time delay axis for f_d=0 are shown in Figures 7 and 8. It can be seen from Figure 7 that the spikes appear at multiples of PRF in the frequency axis. The first null for each spike is $1/(NT_r)$ away from the center of the spike. Therefore, each spike has null to null width of $2/(NT_r)$ along the frequency axis. Amplitudes of those spikes vary as a SINC function. Zero amplitude will appear at $1/T_s$. From Figure 8, there is 2N-1 spikes along the time delay axis. From Eq. 26-1, it is easy to show that the first null for the central spike (p=0) occurrs at $1/(N\Delta f)$. Accordingly, if $1/(N\Delta f)$ is less than pulse width T_s, the stepped frequency radar will have better range resolution than the pulse radar. Plots of cut along the delay axis with different frequency step Δf's are presented in Figure 9. The larger the radar's frequency step, the better the resolution of the radar.

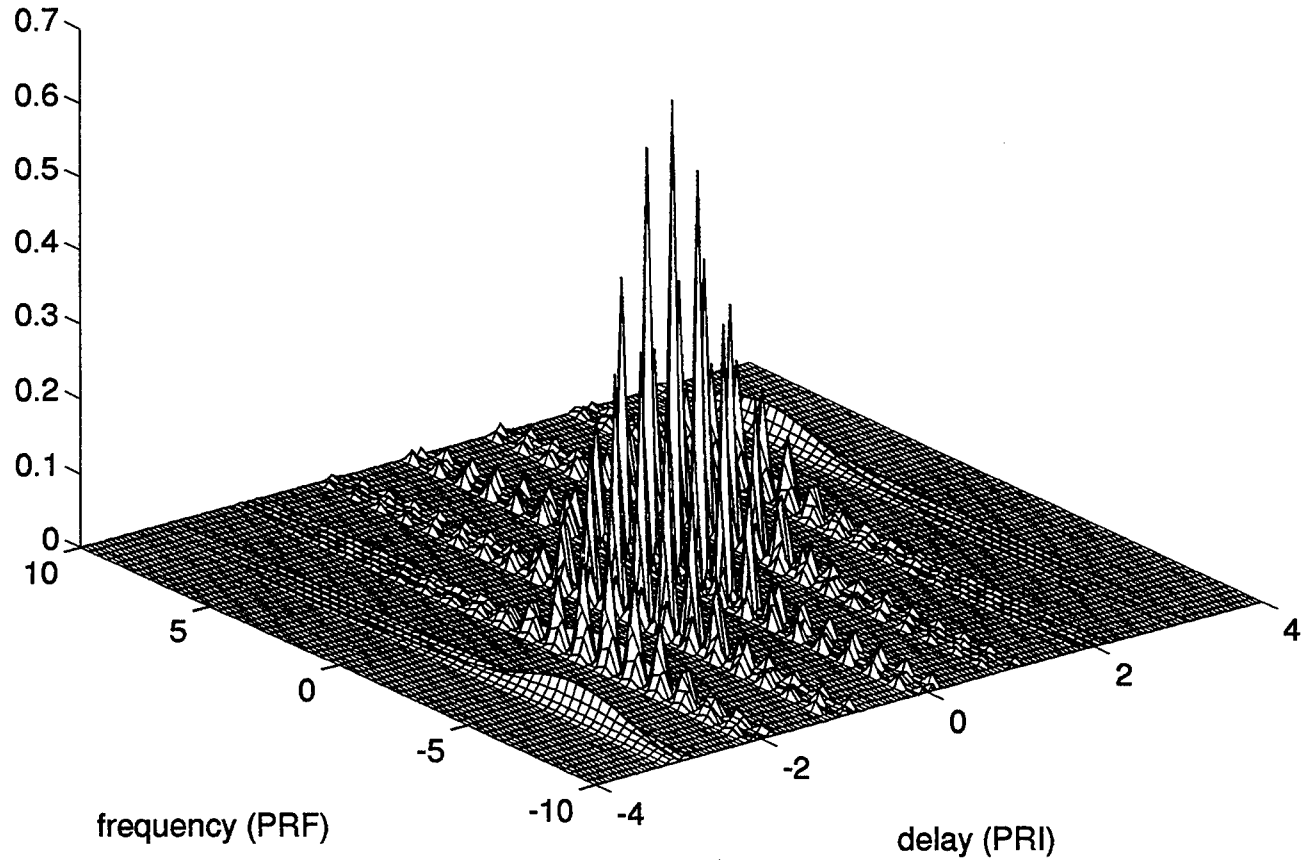

Figure 5. Auto-ambiguity Diagram of the Stepped Frequency Radar, Pulse Number N=4, Duty-cycle=0.2, Δf =2PRF.

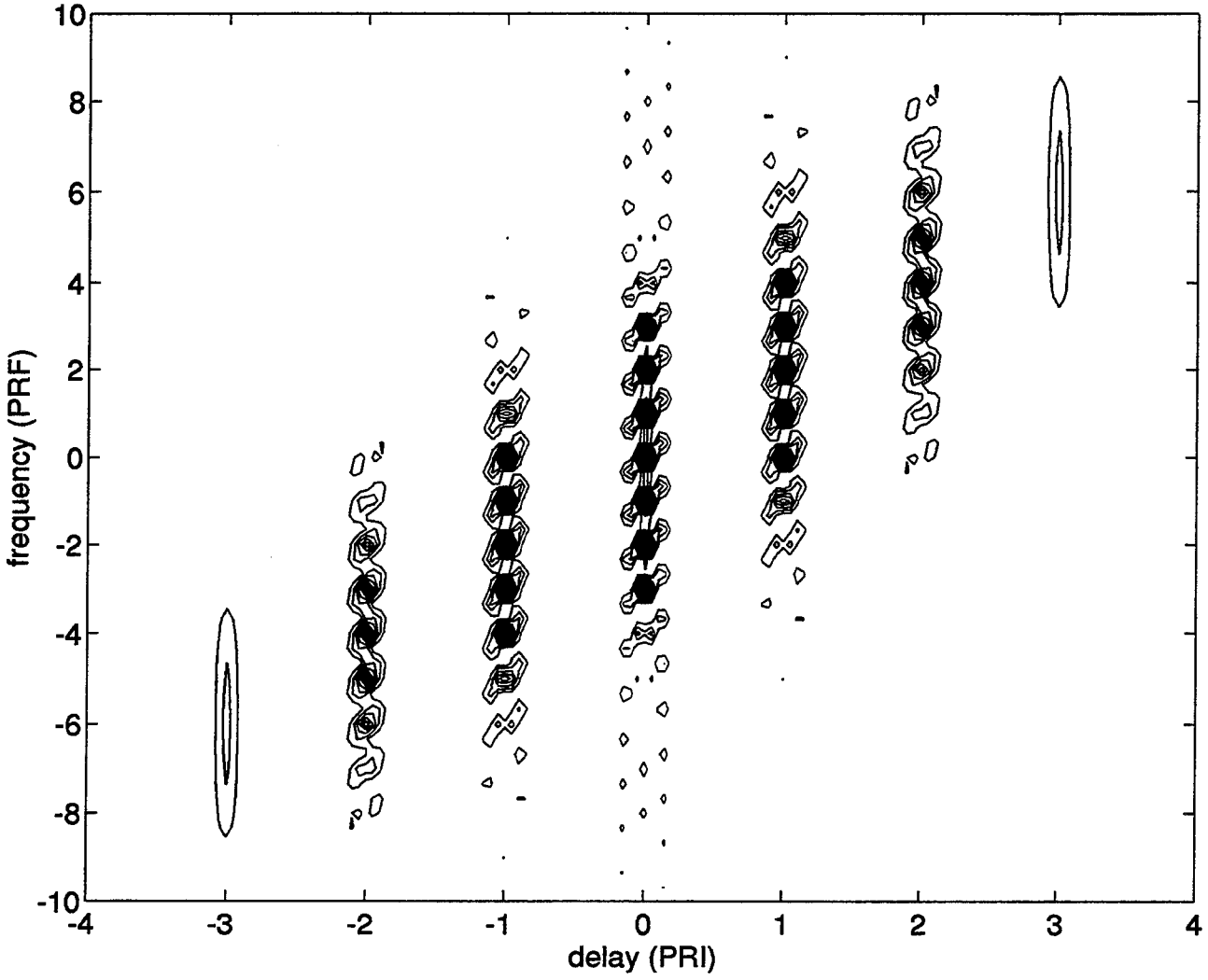

Figure 6. Contour Plot of the Auto-ambiguity Diagram for the Stepped Frequency Radar, Pulse Number N=4, Duty-cycle=0.2 ,Δf =2PRF.

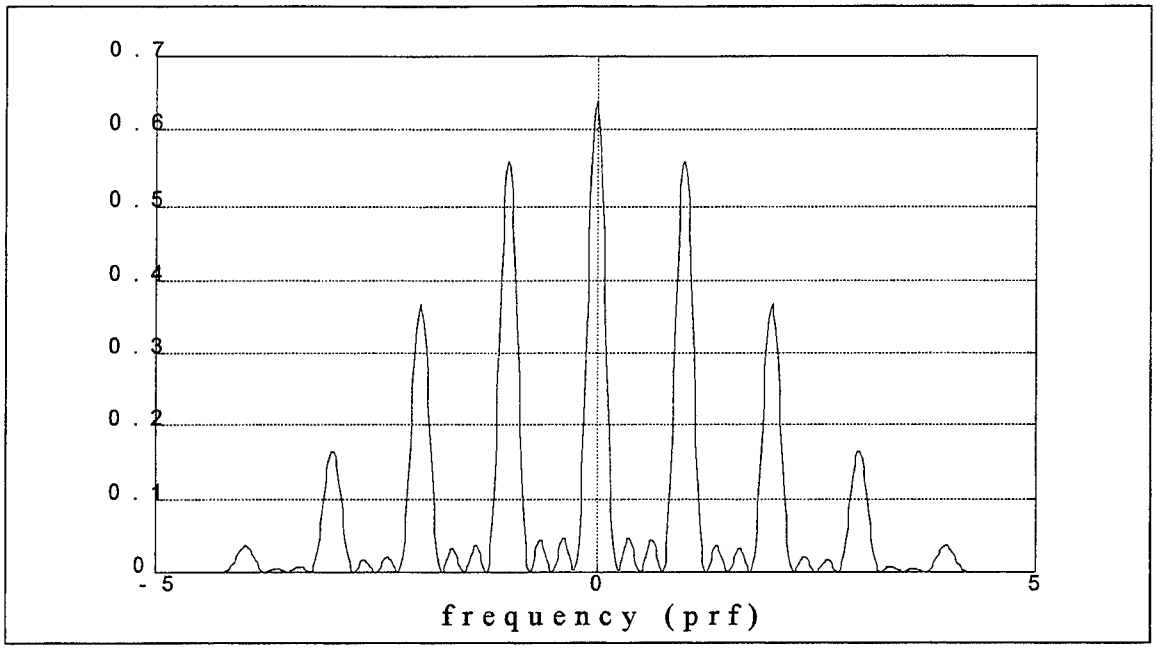

Figure 7. Plot of Cut along the Frequency Axis for $\tau = 0$ of the Auto-ambiguity Function for the Stepped Frequency Radar, Pulse Number N=4, Duty-cycle=0.2 , Δf = 2PRF.

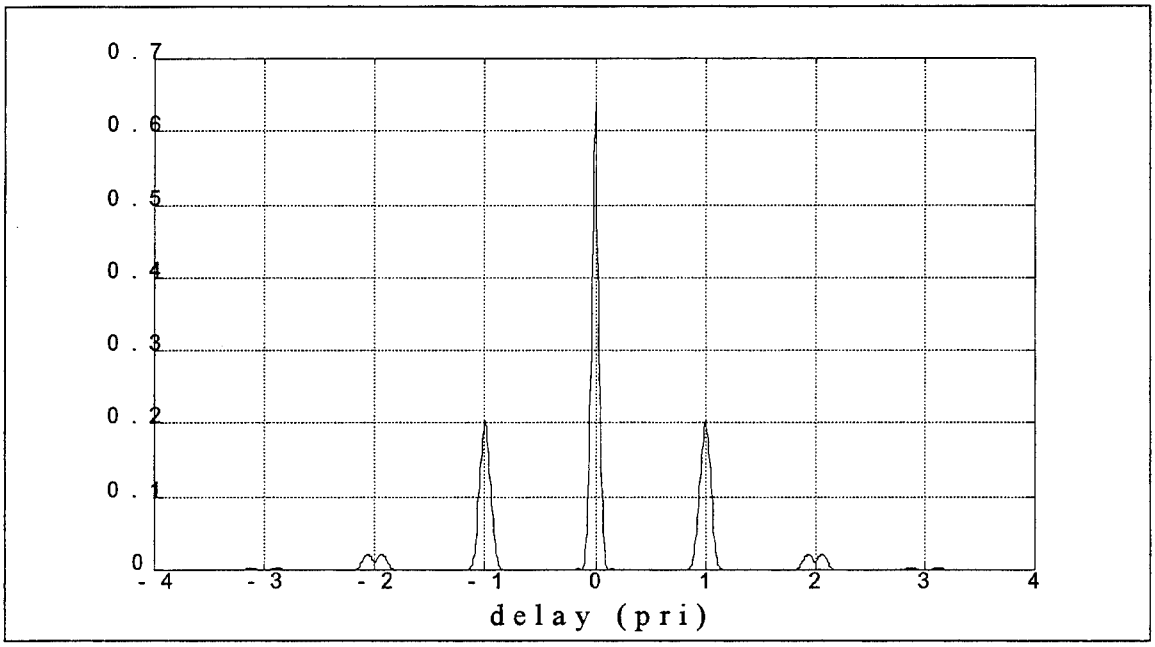

Figure 8. Plot of Cut along the Time Axis for f=0 of the Auto-ambiguity Function for the Stepped Frequency Radar, Pulse Number N=4, Duty-cycle=0.2, Δf =2PRF.

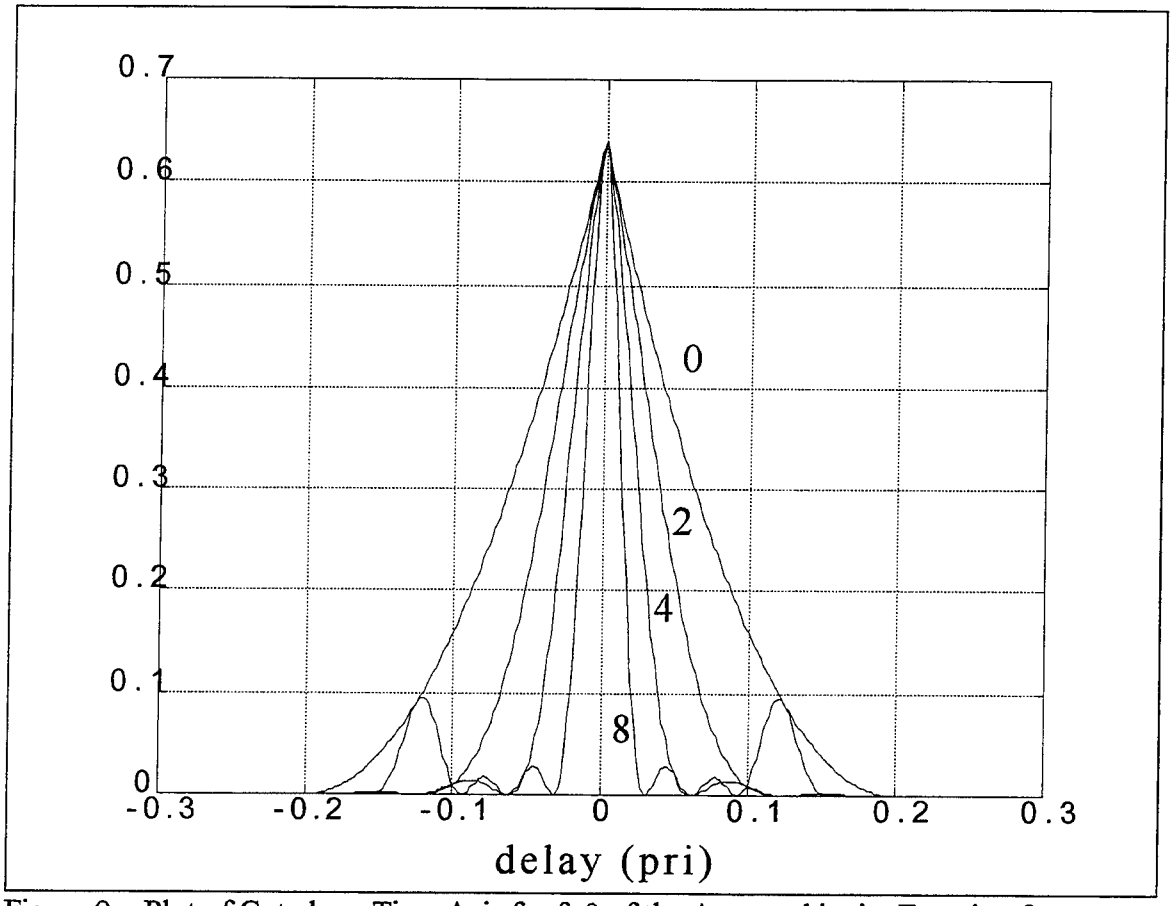

Figure 9. Plot of Cut along Time Axis for f=0 of the Auto-ambiguity Function for the Stepped Frequency Radar, Pulse Number N=4, Duty-cycle=0.2, Δf=[0,2,4,8] PRF.

C. DERIVATION OF THE CROSS-AMBIGUITY FUNCTION FOR THE STEPPED FREQUENCY RADAR

In this section the mathematical expression of the ambiguity function for the stepped frequency radar receiver and processor as shown in Figure 2 are derived. Since the filter used in this system is only matched to the individual pulse instead of matched to the transmitted signal which is composed of N pulses, the ambiguity function of this stepped frequency radar processor is called the cross-ambiguity function. The stepped frequency radar can be mathematically modeled as shown in Figure 10. The transmitted and received signals were defined in Equation 16 and Equation 17 respectively. The received signal is mixed with a local oscillator, stepped frequency synthesizer, and a coherent oscillator. The stepped frequency synthesizer is synchronized so that the transmitter and receiver are on the same frequency step. As a result, multiple time around echoes will have frequencies which vary by multiples of frequency step size Δf. The signal is then passed through a filter which is matched to a single pulse envelope. The output of the pulse-envelope matched filter is sampled and the samples undergo the discrete-time signal processing shown in Figure 10.

The output of the stepped frequency synthesizer used in the receiver is defined as

$$S_{step}(t) = \sum_{n=0}^{N-1} \mu(t - nT_r) e^{-j2\pi(n\Delta f)t}, \tag{27}$$

where

$$\mu(t - nT_r) = \begin{cases} 1, & \text{if } nT_r \le t \le (n+1)T_r, \text{ and} \\ 0, & \text{elsewhere.} \end{cases} \tag{28}$$

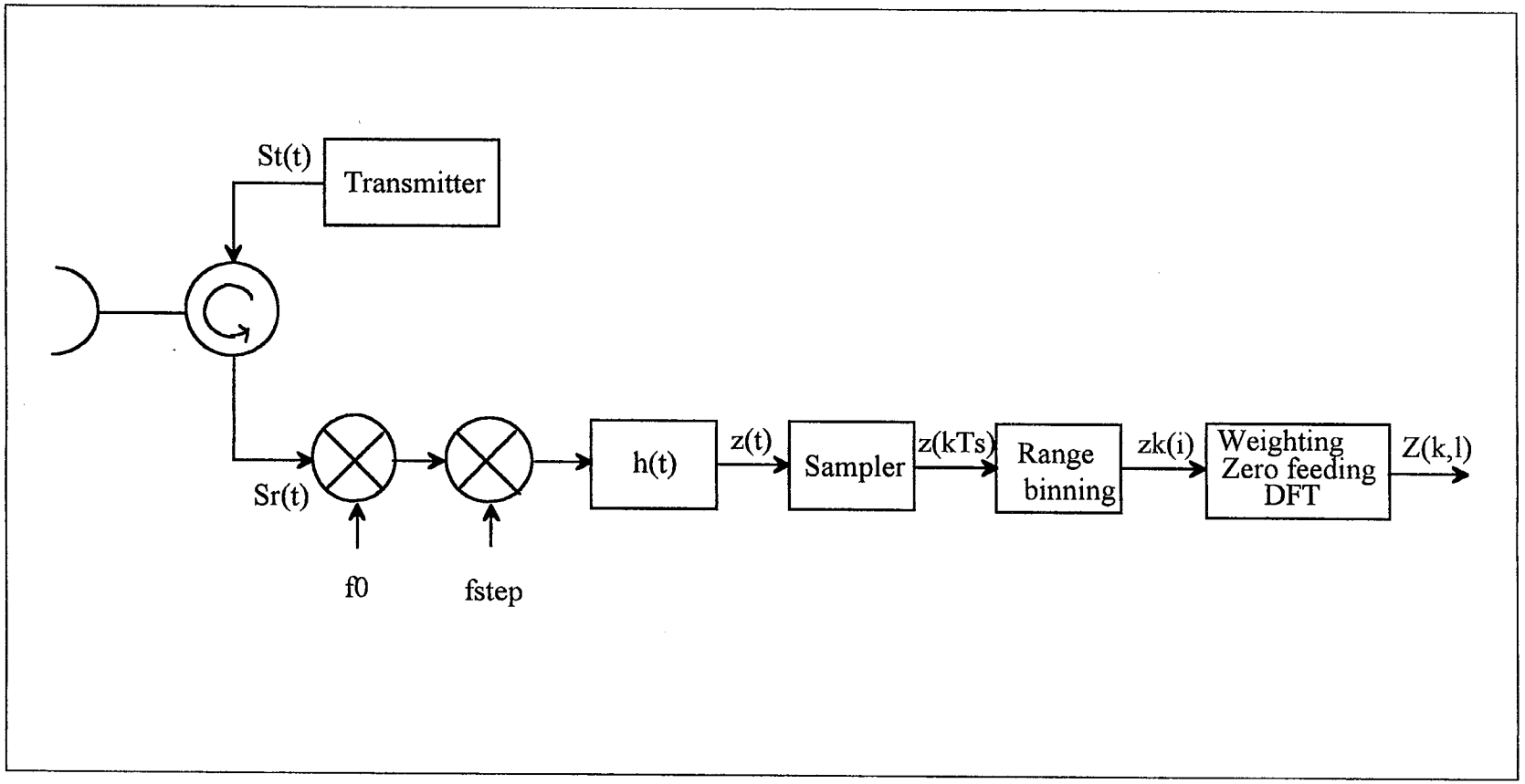

Figure 10. The Mathematical Model of the Stepped Frequency Radar

The output of the matched filter, z(t), can be derived by taking the convolution of the impulse response of the matched filter, h(t), and the received signal at the input of the matched filter. The received signal at the input of the matched filter can be defined as

$$S_i(t) = e^{-j2\pi f_0 t} \times S_{step}(t) \times S_r(t) . \tag{29}$$

The output of the matched filter can then be expressed as

$$z(t_0) = \int_{-\infty}^{\infty} S_i(\eta) \times h^*(t_0 - \eta) d\eta$$

$$= \int_{-\infty}^{\infty} e^{-j2\pi f_0 \eta} \times \left(\sum_{m=0}^{N-1} \mu(\eta - mT_r) e^{-j2\pi m \Delta f \eta} \right)$$

$$\times \left(a_r \sum_{n=0}^{N-1} u(\eta - \tau - nT_r) e^{j2\pi (f_0 + f_d + n\Delta f)(\eta - \tau)} \right) \times h^*(t_0 - \eta) d\eta . \tag{30}$$

The above equation can be rewritten as

$$z(t_0) = a_r \int_{-\infty}^{\infty} e^{-j2\pi f_0 \tau} \times e^{j2\pi f_d (\eta - \tau)} \times J \times h^*(t_0 - \eta) d\eta , \tag{31}$$

where

$$J = \sum_{m=0}^{N-1} \mu(\eta - mT_r) e^{-j2\pi m \Delta f \eta} \times \sum_{n=0}^{N-1} u(\eta - \tau - nT_r) e^{j2\pi n \Delta f (\eta - \tau)} , \tag{32}$$

and τ is defined in Equation 22.

If each pulse of the received signal is assumed to fall within the same pulse of the stepped frequency signal no matter how τ varies, then J can be expressed as

$$J = e^{-j2\pi\kappa\Delta f\eta} \sum_{n=\max(0,-p)}^{\min(N-1-p,N-1)} u(\eta-\tau-nT_r)e^{-j2\pi n\Delta f\tau}, \tag{33}$$

where $\kappa = p, \quad$ if $pT_r < \tau < (p+1)T_r - T_s,$

$= p+1, \quad$ if $(p+1)T_r - T_s < \tau < (p+1)T_r.$ (34)

Substituting Equation 33 into Equation 31, we obtain the output of the matched filter as

$$z(t_0) = a_r e^{-j2\pi(f_0+f_d)\tau} \times \int_{-\infty}^{\infty} e^{j2\pi(f_d-\kappa\Delta f)\eta} \times$$

$$\sum_{n=\max(0,-p)}^{\min(N-1-p,N-1)} u(\eta-\tau-nT_r)e^{-j2\pi n\Delta f\tau} \times h^*(t_0-\eta)d\eta. \tag{35}$$

Letting $\xi = \eta - t_0$, we rewrite the output of the matched filter as

$$z(t_0) = a_r e^{-j2\pi(f_0+f_d)\tau} \times e^{j2\pi(f_d-\kappa\Delta f)t_0}$$

$$\times \int_{-\infty}^{\infty} e^{j2\pi(f_d-\kappa\Delta f)\xi} \left[\sum_{n=\max(0,-p)}^{\min(N-1-p,N-1)} u(\xi+t_0-\tau-nT_r) \right] \times h^*(-\xi)d\xi$$

$$= a_r e^{-j2\pi(f_0+f_d)\tau} \times e^{j2\pi f_m t_0} \times \int_{-\infty}^{\infty} e^{j2\pi f_m\xi} \times V(\xi-(\tau-t_0),\tau) \times h^*(-\xi)d\xi, \tag{36}$$

where $f_m = f_d - \kappa\Delta f$, (37)

$$V(t,\tau) = \sum_{n=\max(0,-p)}^{\min(N-1-p,N-1)} u(t-nT_r)e^{-j2\pi n\Delta f\tau}. \tag{38}$$

It is customary to set t_0 to 0 for the computation of the ambiguity function and neglect the first exponential term, since we are only interested in the magnitude of the matched filter outputs. Redefining the output of the matched filter $z(t_0)$ as $X(\tau,f_m)$, we obtain the output of the matched filter as

$$X(\tau,f_m)=\int_{-\infty}^{\infty} e^{j2\pi f_m t}\times V(t-\tau,\tau)\times h^*(-t)dt. \qquad (39)$$

According to the definition of the ambiguity function in Equation 8, we treat f_m as the frequency shift of signal at the input of the matched filter. This frequency shift consists of the Doppler shift and the frequency changes due to the stepped frequency waveform. $V(t,\tau)$ is then the envelope of signal at the input of the matched filter. Thus $X(\tau,f_m)$ becomes the cross-ambiguity function of the stepped frequency radar without the processor. In this form a positive τ indicates a target beyond the reference delay t_0.

In the rest of the section, the ambiguity function is extended to include the signal processor. The matched filter output is sampled at instants $t=nT_s$ and the samples undergo discrete-time signal processing. The sample rate, $1/T_s$, is greater than or equal to the bandwidth of the pulse envelope u(t). Further, the pulse repetition interval (PRI), T_r, is an integer multiple, k, of T_s. The sample stream for all the pulses is sorted into k parallel processing streams termed ambiguous range bins. Processing within each range bin utilizes only samples from time instants separated by integer multiples of T_r. [Ref. 6]

The ith sample for range bin k can be defined as

$$z_k(i) = z(kT_s + iT_r). \tag{40}$$

These samples from the matched filter output which are associated with a range bin are processed together by a discrete Fourier transformation (DFT) processor. A Hamming window is applied before executing the DFT to reduce frequency sidelobes. Out of N samples in a range bin, the first I samples are rejected to allow for the settling of transients due to range ambiguous clutter [Ref. 7]. DFT is taken as the last M weighted samples of each range bin as given below

$$Z(k,l) = \sum_{i=0}^{M-1} w(i) e^{-j2\pi i \frac{l}{M}} z_k(i+I), \tag{41}$$

where

k : range bin index,
l : Doppler filter index,
M : the number of samples that DFT processed, and $M < N - |p|$,
i : sample index, i=0,1,...,M-1,
w : the window coefficients,
I : the number of samples that will be rejected initially.

Substituting Equations 35 and 40 into Equation 41, we obtain the lth output of the DFT for range bin k as

$$Z(k,l) = a_r e^{-j2\pi(f_0+f_d)\tau} \times$$

$$\int_{-\infty}^{\infty} e^{j2\pi f_m \eta} \sum_{n=\max(0,-p)}^{\min(N-1-p,N-1)} u(\eta - \tau - nT_r) e^{-j2\pi n \Delta f \tau} \times h_l^*(kT_s - \eta) d\eta , \tag{42}$$

where

$$h_l^*(t) = \sum_{i=0}^{M-1} w(i) e^{-j2\pi i \frac{l}{M}} h^*(t + (i+I)T_r). \tag{43}$$

$h^*_l(t)$ is the impulse response of the radar receiver processor which includes the pulse envelope matched filter, weighting function and Doppler processor .

Equation 42 has the same form that Equation 35 does. So after changing variables, setting kT_s equal to zero and neglecting the first exponential term, the lth output of DFT can be written as

$$X_l(\tau, f_m) = \int_{-\infty}^{\infty} e^{j2\pi f_m t} V(t-\tau, \tau) h_l^*(-t) dt, \tag{44}$$

The above equation defines the cross-ambiguity function associated with the mathematical model of the stepped frequency radar processor as illustrated in Figure 10. The subscript l indicates that a distinct ambiguity function is defined for each Doppler filter.

For the received pulse to be matched to the transmitted pulse, h(t) should be equal to $\mu(-t)$. From Equations 37, 42, and 43, after simplifying, the ambiguity function for lth DFT can be expressed as

$$X_l(\tau, f_d) = \sum_{i=\max(0,p-l)}^{\min(N-1-l+p, N-1-l, M-1)} w(i) \times e^{-j2\pi i \frac{l}{M}} \times e^{-j2\pi(l+i-p)\Delta f \tau} \times e^{j2\pi(f_d - \kappa\Delta f)(i+l)T_r}$$

$$\times (T_s - \gamma T_r) \times e^{j\pi(f_d - \kappa\Delta f)(T_s + \gamma T_r)} \times \frac{\sin \pi(f_d - \kappa\Delta f)(T_s - \gamma T_r)}{\pi(f_d - \kappa\Delta f)(T_s - \gamma T_r)},$$

$$\text{for } 0 \le \gamma < \frac{T_s}{T_r}, \tag{45-1}$$

$$X_l(\tau,f_d)=\sum_{i=\max(0,p+1-l)}^{\min(N-l+p,N-l,M-1)} w(i)\times e^{-j2\pi i\frac{l}{M}}\times e^{-j2\pi(l+i-p-1)\Delta f\tau}\times e^{j2\pi(f_d-\kappa\Delta f)(i+l)T_r}$$

$$\times(T_s+(\gamma-1)T_r)\times e^{j\pi(f_d-\kappa\Delta f)(T_s+(\gamma-1)T_r)}\times\frac{\sin\pi(f_d-\kappa\Delta f)(T_s+(\gamma-1)T_r)}{\pi(f_d-\kappa\Delta f)(T_s+(\gamma-1)T_r)},$$

$$\text{for } 1-\frac{T_s}{T_r}\le\gamma<1, \qquad (45\text{-}2)$$

$$=0, \qquad \text{elsewhere.} \qquad (45\text{-}3)$$

Taking the absolute value of the above equation, we obtain the ambiguity function as

$$|X_l(\tau,f_d)|=(T_s-\gamma T_r)\times\left|\frac{\sin\pi(f_d-p\Delta f)(T_s-\gamma T_r)}{\pi(f_d-p\Delta f)(T_s-\gamma T_r)}\right|\times$$

$$\left|\sum_{i=\max(0,p-l)}^{\min(N-1-l+p,N-1-l,M-1)} w(i)\times e^{-j2\pi i\frac{l}{M}}\times e^{j2\pi(f_d-(2p+\gamma)\Delta f)iT_r}\right|,$$

$$\text{for } 0\le\gamma<\frac{T_s}{T_r}, \qquad (46\text{-}1)$$

$$=(T_s+(\gamma-1)T_r)\times\left|\frac{\sin\pi(f_d-(p+1)\Delta f)(T_s+(\gamma-1)T_r)}{\pi(f_d-(p+1)\Delta f)(T_s+(\gamma-1)T_r)}\right|\times$$

$$\left|\sum_{i=\max(0,p+1-l)}^{\min(N-l+p,N-l,M-1)} w(i)\times e^{-j2\pi i\frac{l}{M}}\times e^{j2\pi(f_d-(2p+\gamma+1)\Delta f)iT_r}\right|,$$

$$\text{for } 1-\frac{T_s}{T_r}\le\gamma<1, \qquad (46\text{-}2)$$

$$=0, \qquad \text{elsewhere.} \qquad (46\text{-}3)$$

The above equation becomes the cross-ambiguity function of the stepped frequency radar processor. The cross-ambiguity function can describe the auto-ambiguity

function of the stepped frequency radar by setting the Doppler filter index l to zero and assuming a uniform window, w(i)=1, setting I to zero, and setting the number of transmitted pulses, N, equal to the number of samples processed, M. Under these assumptions and after simplifying, the ambiguity function becomes

$$|X_0(\tau,f_d)| = (T_s-\gamma T_r)\times\left|\frac{\sin\pi(f_d-p\Delta f)(T_s-\gamma T_r)}{\pi(f_d-p\Delta f)(T_s-\gamma T_r)}\right|\times\left|\frac{\sin\pi(f_d-(2p+\gamma)\Delta f)(N-|p|)T_r}{\sin\pi(f_d-(2p+\gamma)\Delta f)T_r}\right|,$$

$$\text{for } 0\le\gamma<\frac{T_s}{T_r}, \qquad (47\text{-}1)$$

$$=(T_s+(\gamma-1)T_r)\times\left|\frac{\sin\pi(f_d-(p+1)\Delta f)(T_s+(\gamma-1)T_r)}{\pi(f_d-(p+1)\Delta f)(T_s+(\gamma-1)T_r)}\right|\times\left|\frac{\sin\pi(f_d-(2p+\gamma+1)\Delta f)(N-|p+1|)T_r}{\sin\pi(f_d-(2p+\gamma+1)\Delta f)T_r}\right|,$$

$$\text{for } 1-\frac{T_s}{T_r}\le\gamma<1, \qquad (47\text{-}2)$$

$$=0, \qquad \text{elsewhere.} \qquad (47\text{-}3)$$

The above equation is exactly the same as the expression of the auto-ambiguity function in Equation 24. If we let the frequency step, Δf, be zero, it is easy to prove that Equation 38 becomes the ambiguity function of a pulse train as expressed in Appendix A Equation. A.13.

The ambiguity diagram of the 0th, l=0, Doppler filter of the stepped frequency radar with a Hamming window in the Doppler processor is illustrated in Figure 11. Figures 12 and 13 are plots of cut along the frequency axis and delay axis respectively. From the comparison of Figures 12 and 13 with Figures 7 and 8 which are the cut plots of the

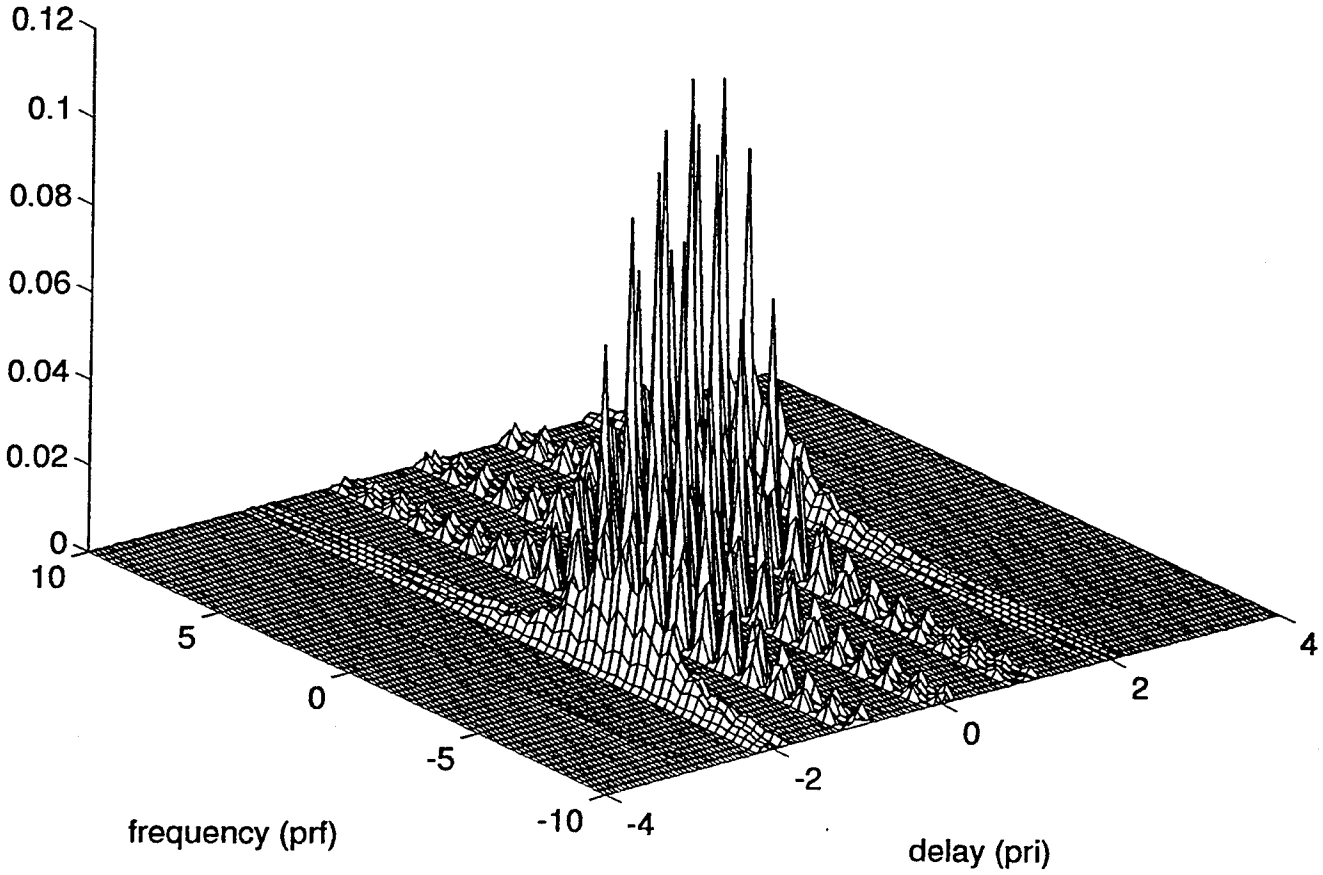

Figure 11. Cross-ambiguity Diagram of the Stepped Frequency Radar, Pulse Number N=4, Number of Pulses Processed M=4, Duty-cycle=0.2, Δf =2PRF, I=0, l=0, and with Hamming Window

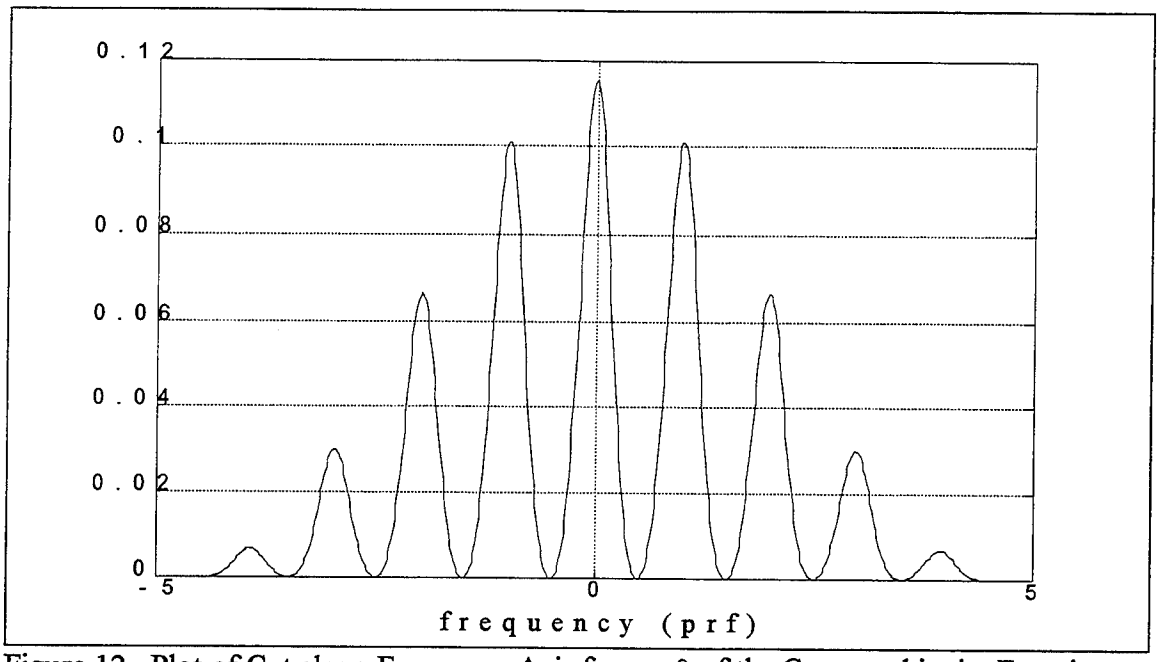

Figure 12. Plot of Cut along Frequency Axis for $\tau = 0$ of the Cross-ambiguity Function for the Stepped Frequency Radar , Pulse Number N=4, Number of Pulses Processed M=4, Duty cycle=0.2, Δf =2PRF, I=0, l=0, and with Hamming Window

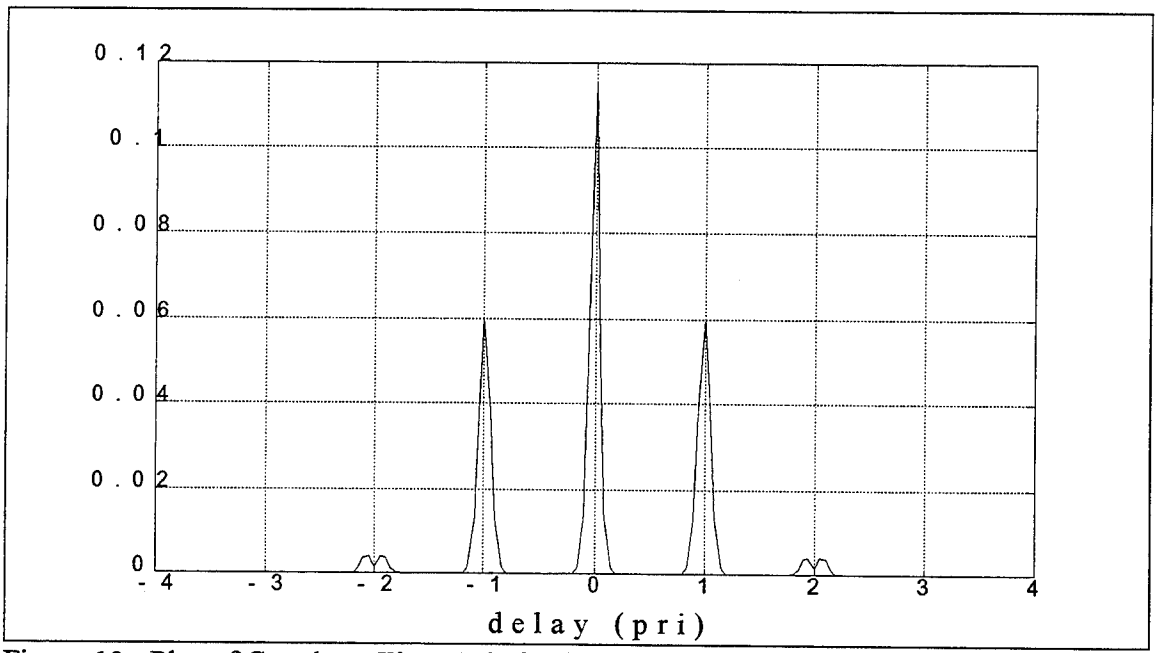

Figure 13. Plot of Cut along Time Axis for f=0 of the Cross-ambiguity Function for the Stepped Frequency Radar, Pulse Number N=4, Number of Pulses Processed M=4, Duty-cycle=0.2 ,Δf =2PRF , I=0, and l=0, and with Hamming Window

auto-ambiguity diagram for the stepped frequency radar without window function, one can find that window functions which are often used in radar processors will decrease the amplitude of each spike and spread the width of it in return for reducing the sidelobes of each spike. The decrease in amplitude will reduce the detection capability and the spread of the width of the spike will cause poor accuracy and resolution. On the other hand, reducing the sidelobe of the spike will enhance the detection of small targets close to the large target. Figure 14 shows the bank of Doppler filters within a DFT processor . This figure indicates that the ambiguity function for the lth Doppler filter is the shifted version, along the frequency axis, of the ambiguity function for the 0th Doppler filter. The effect of decay for different Doppler filters is caused by the window function.

The improvement in clutter suppression capability that is achieved using pulse Doppler processing, including the use of rejecting I pulses for initialization, is demonstrated in Figures 15 thru 28 [Ref. 7]. The figures were drawn using the MATLAB computer program which calculates the ambiguity function defined by Equation 47. Figures 15 thru 22 show the clutter suppression capability for the pulse radar, and Figures 23 thru 28 show the clutter suppression capability for the stepped frequency radar. In all these plots, the sample step of time delay axis is 4 PRI. Therefore only envelopes of the ambiguity diagram are shown in the time delay axis. In the frequency shift axis, there are many spikes occurring at the position of multiples of PRF, but only a single spike is shown in the plots. The Hamming window is used in all of these plots. In Figures 15, 17, 19, 21, 23, 25, and 28, the number of transmitted pulses and processed pulses are equal,

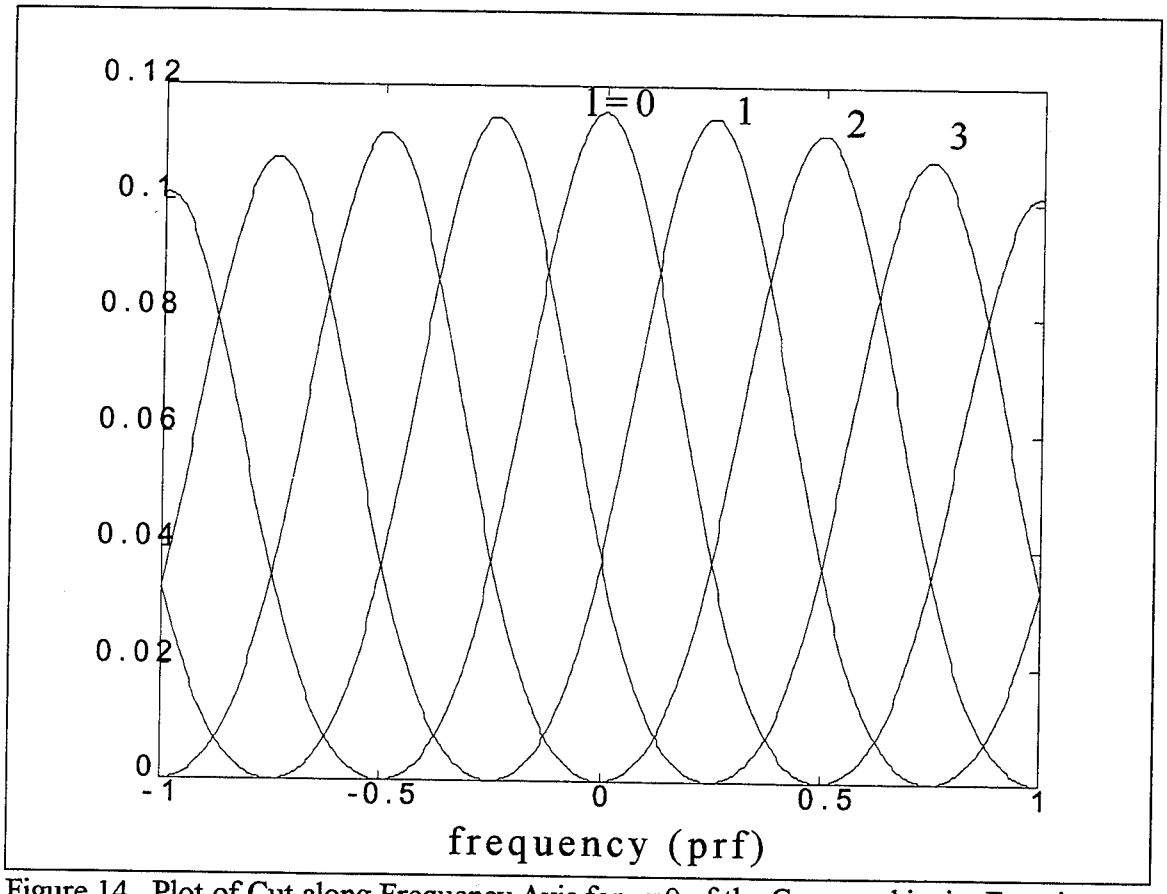

Figure 14. Plot of Cut along Frequency Axis for τ=0 of the Cross-ambiguity Function for the Stepped Frequency Radar, Pulse Number N=4, Number of Pulses Processed M=4, Duty cycle=0.2 , Δf.=2PRF, I=0, l=[0,1,2,3], and with Hamming Window

N=M=100, and the number of initial pulses rejected, I, is set to zero. In Figures 16, 18, 20, 22, 24, 26, and 28, the number of transmitted pulses, N, is increased to 150, and I is set to 50. From Figures 15 thru 18, in the case of the pulse radar, the use of initial pulse rejection leads to an ambiguity function which, along the delay axis, is a cross correlation of envelope functions of unequal length. This phenomenon is not clear for the stepped frequency radar due to the different pulse frequencies as shown in Figures 23 and 24. Comparing Figures 19, 21, 25, and 27 with Figures 20, 22, 26, and 28, respectively, the improvement in clutter suppression capability when utilizing initial pulse rejection is clearly demonstrated. Comparison of Figures 19 and 25 with Figures 20 and 26 shows that the clutter in the 0 to 50 PRI range will be rejected by the use of an initial pulse rejection for a 0.1 PRF Doppler mismatch. Figures 21 and 27 show that, without initial pulse rejection, the capability of Doppler processing to suppress clutter is severely degraded when placing 30 PRIs of delay (from the matched delay) when compared to the cases shown in Figures 22 and 28. [Ref. 6]

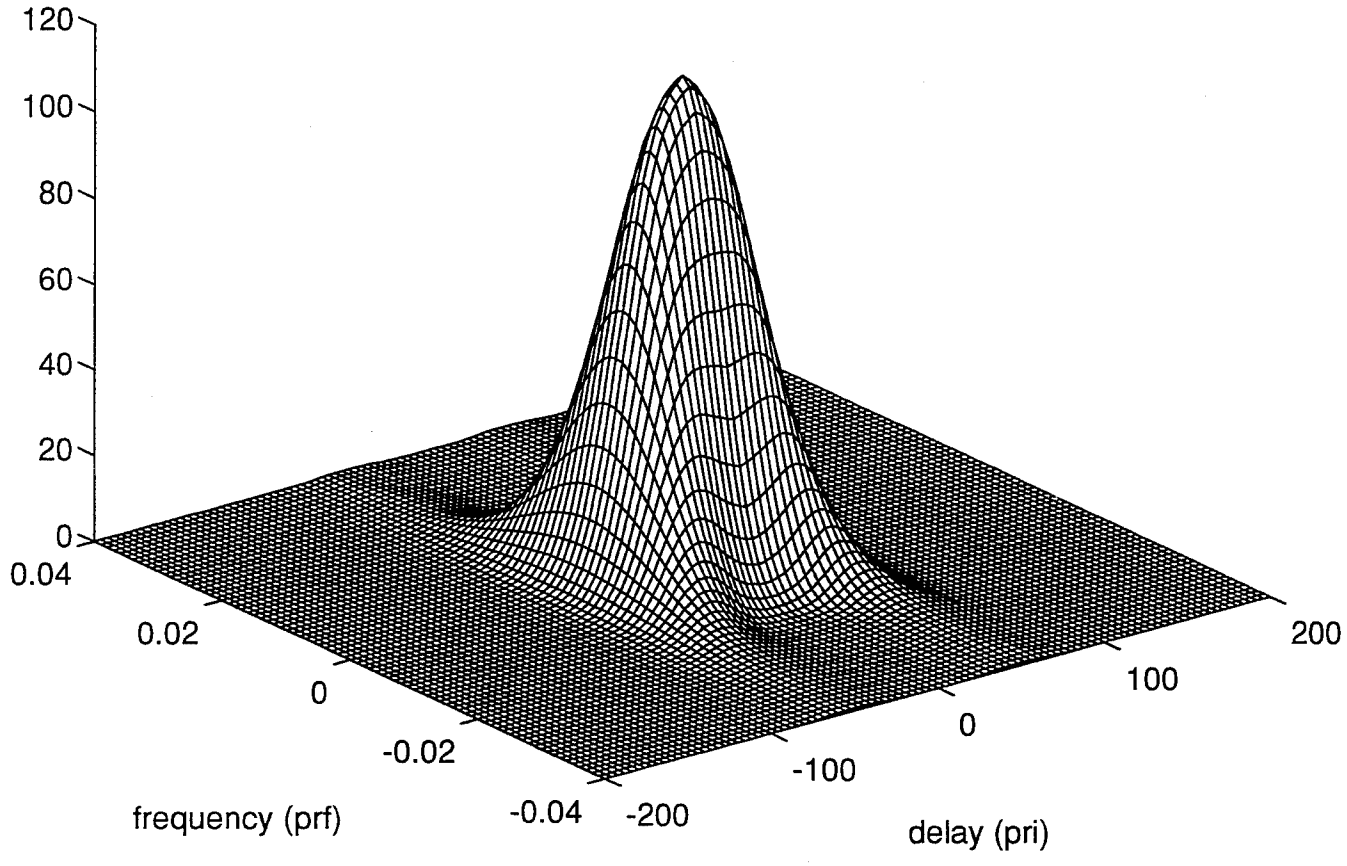

Figure 15. Cross-ambiguity Diagram of the Pulse Radar, Pulse Number N=100, Number of Pulses Processed M=100, Duty-cycle=0.2, Δf =0, I=0, l=0, and with Hamming Window

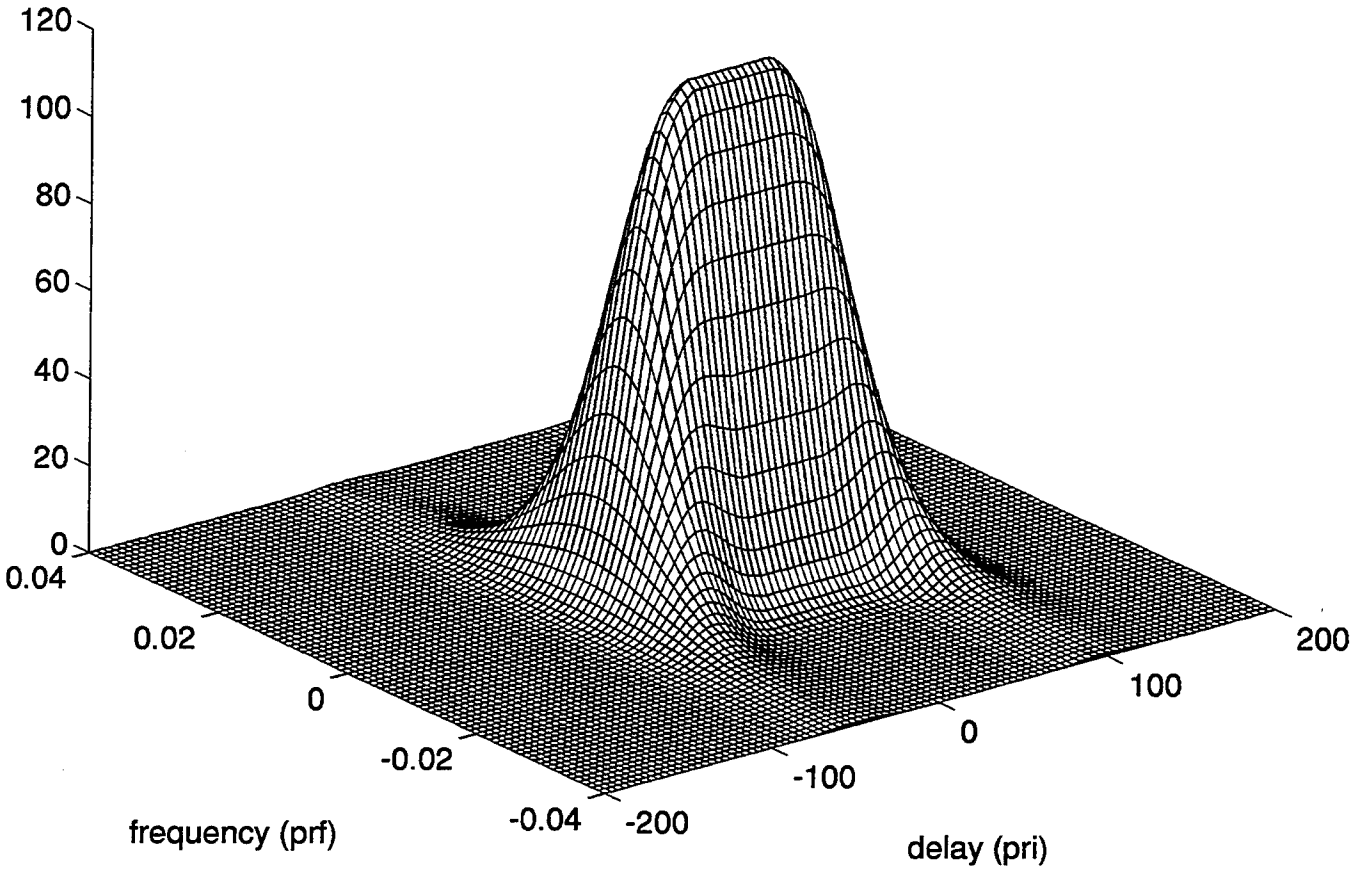

Figure 16. Cross-ambiguity Diagram of the Pulse Radar, Pulse Number N=150, Number of Pulses Processed M=100, Duty-cycle=0.2, Δf =0, I=50, l=0, and with Hamming Window.

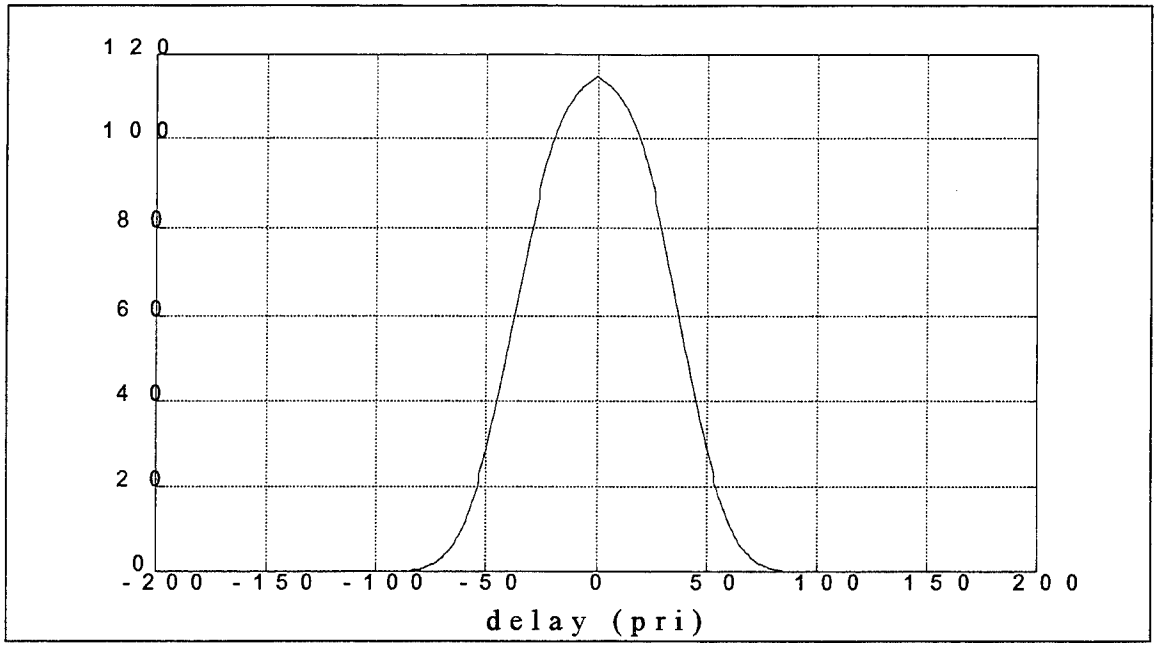

Figure 17. Plot of Cut along Time Axis for f=0 of the Cross-ambiguity Function for the Pulse Radar, Pulse Number N=100, Number of Pulses Processed M=100, Duty cycle=0.2, $\Delta f = 0$, I=0, l=0, and with Hamming Window.

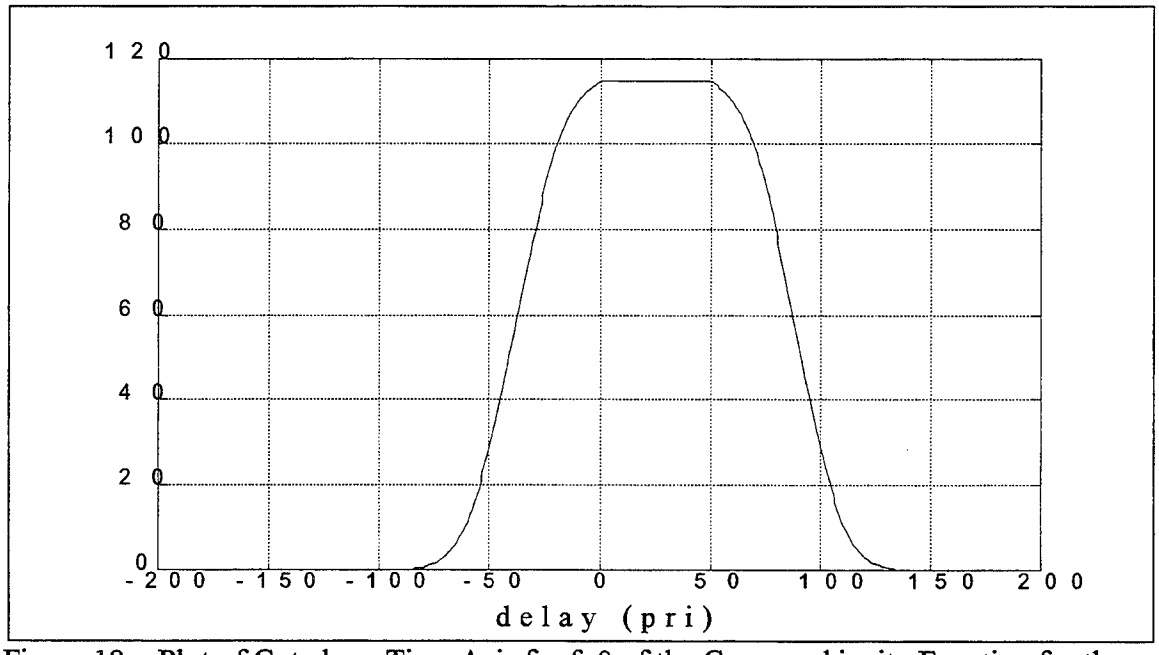

Figure 18. Plot of Cut along Time Axis for f=0 of the Cross-ambiguity Function for the Pulse Radar, Pulse Number N=150, Number of Pulses Processed M=100, Duty-cycle=0.2, Δf =0, I=50, l=0, and with Hamming Window

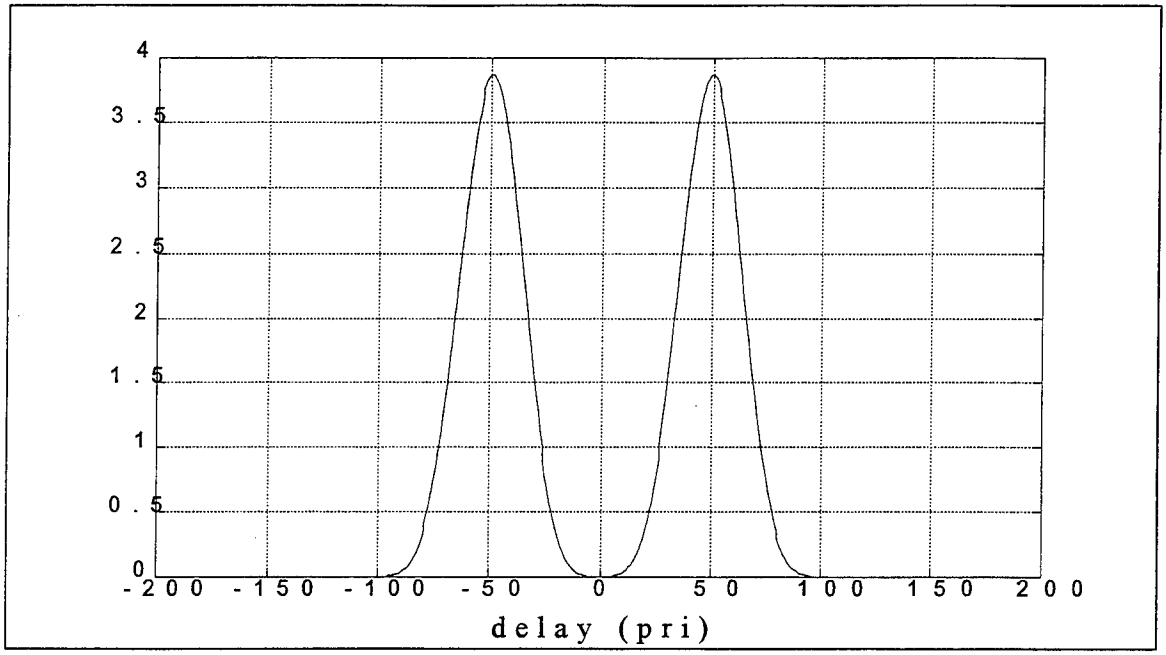

Figure 19. Plot of Cut Parallel to Time Axis for f=0.02PRF of the Cross-ambiguity Function for the Pulse Radar, Pulse Number N=100, Number of Pulses Processed M=100, Duty-cycle=0.2, $\Delta f = 0$, I=0, l=0, and with Hamming Window

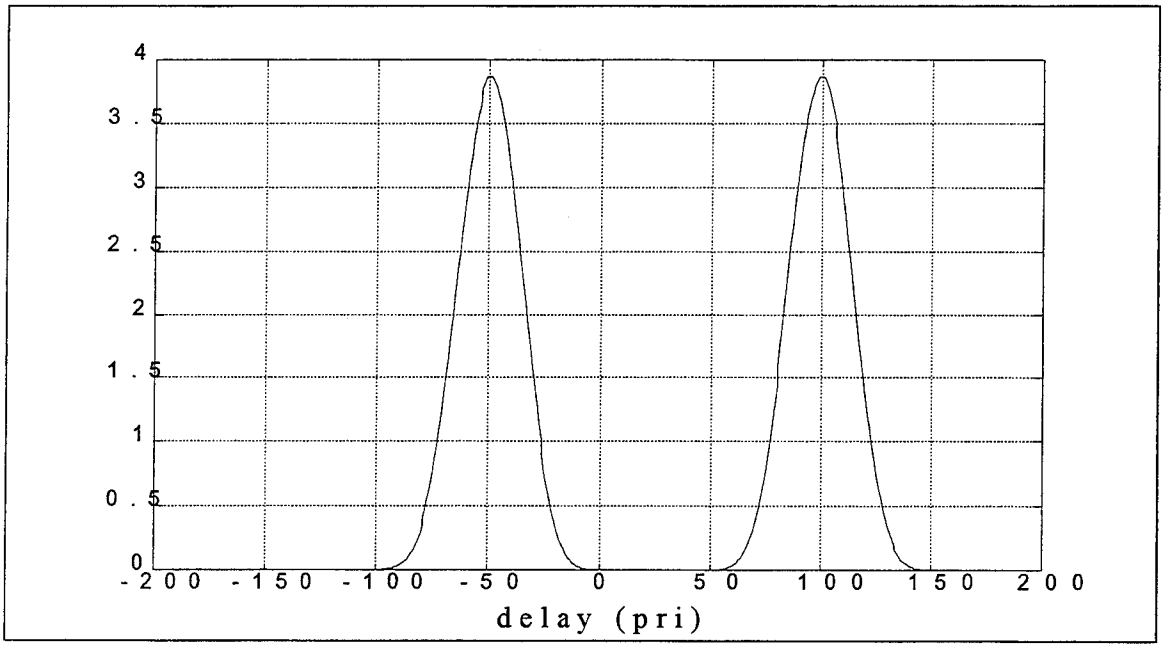

Figure 20. Plot of Cut Parallel to Time Axis for f=0.02PRF of the Cross-ambiguity Function for the Pulse Radar, Pulse Number N=150, Number of Pulses Processed M=100, Duty-cycle=0.2, Δf =0, I=50, l=0, and with Hamming Window.

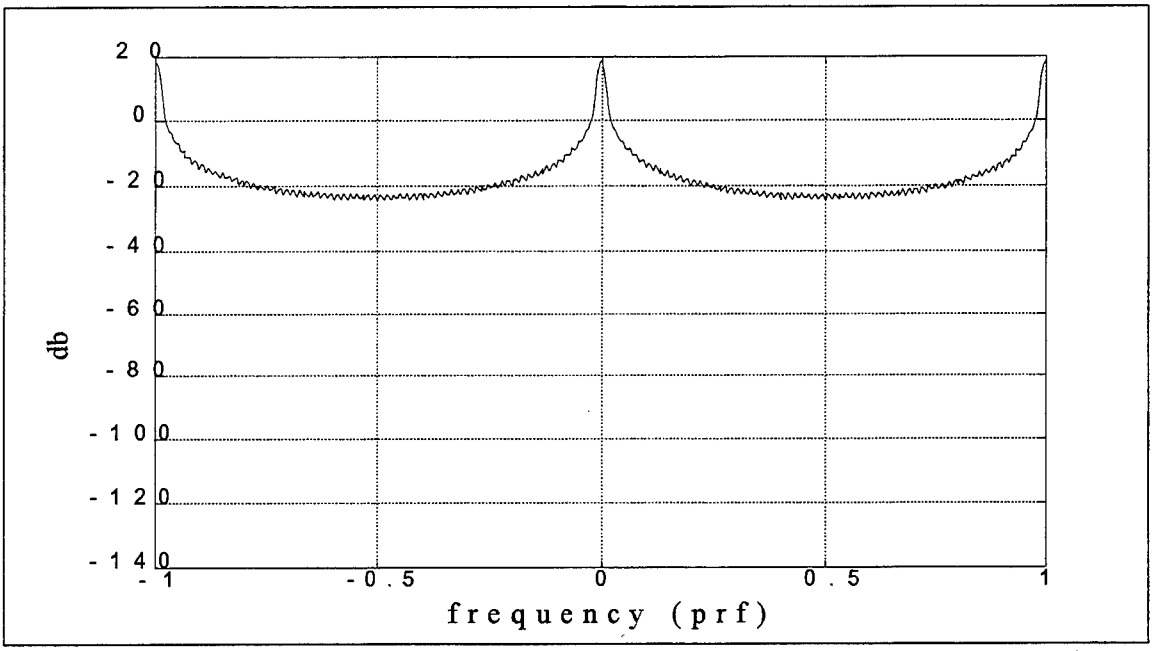

Figure 21. Plot of Cut Parallel to Frequency Axis for τ =30PRI of the Cross-ambiguity Function for thePulse Radar, Pulse Number N=100, Number of Pulses Processed M=100, Duty-cycle=0.2, $\Delta f = 0$, I=0, l=0, and with Hamming Window

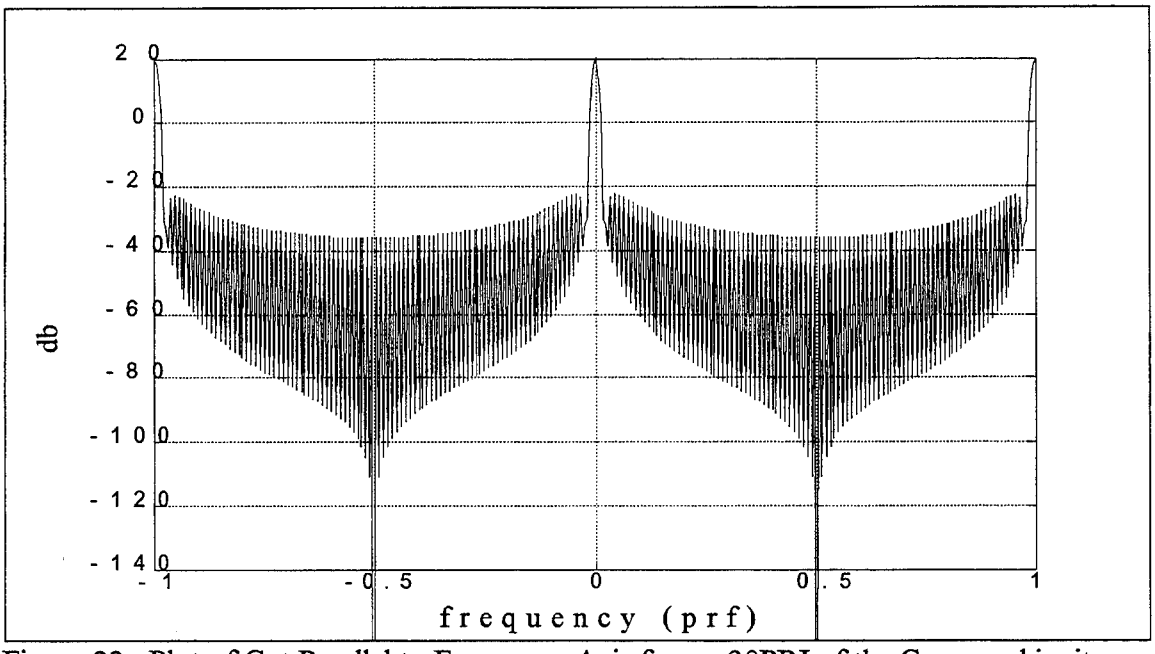

Figure 22. Plot of Cut Parallel to Frequency Axis for τ =30PRI of the Cross-ambiguity Function for the PulseRadar, Pulse Number N=150, Number of Pulses Processed M=100, Duty-cycle=0.2, Δf =0, I=50, l=0, and with Hamming Window.

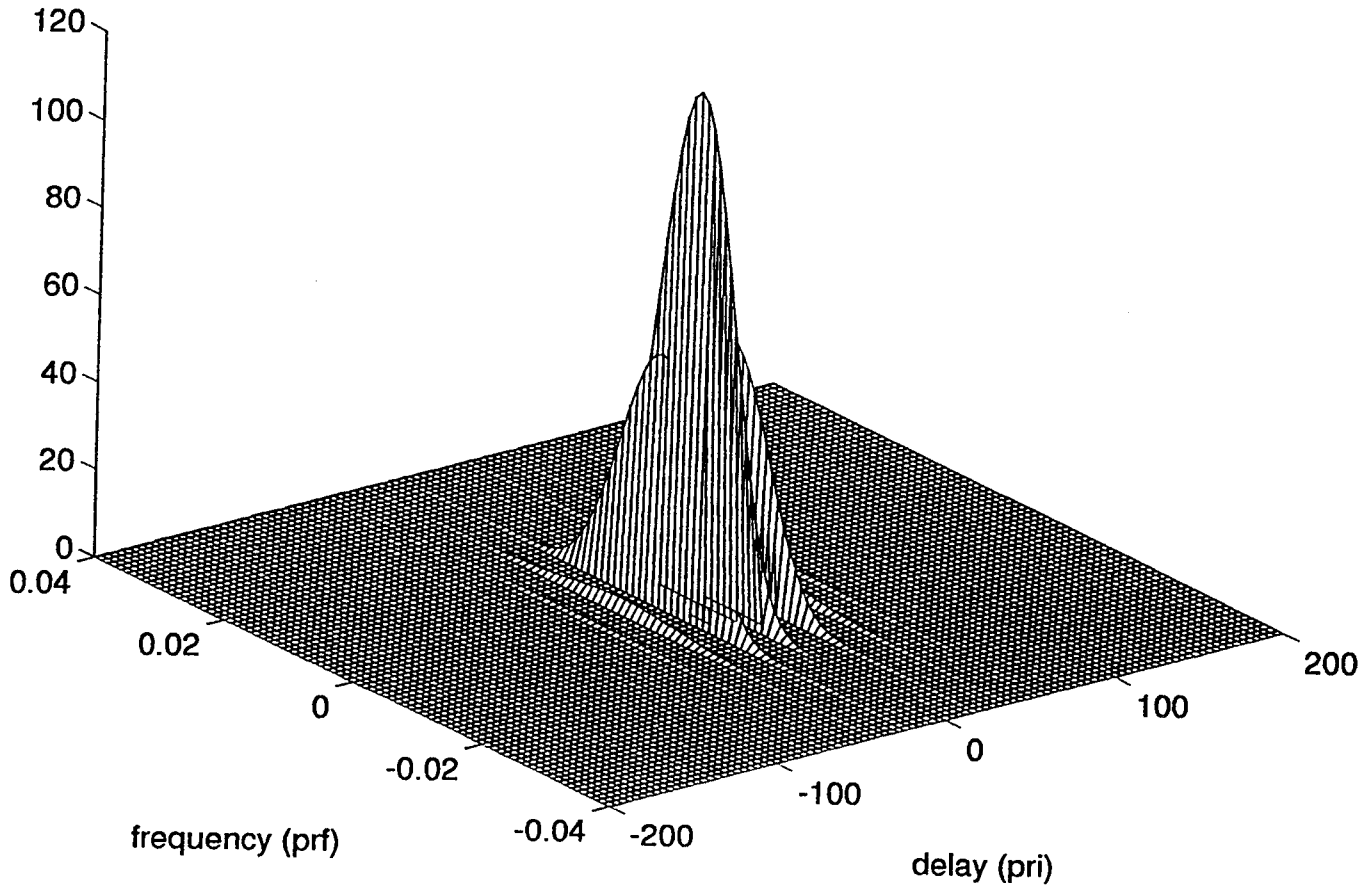

Figure 23. Cross-ambiguity Diagram of the Stepped Frequency Radar, Pulse Number N=100, Number of Pulses Processed M=100, Duty-cycle=0.2 , Δf =0.1PRF, I=0, l=0, and with Hamming Window

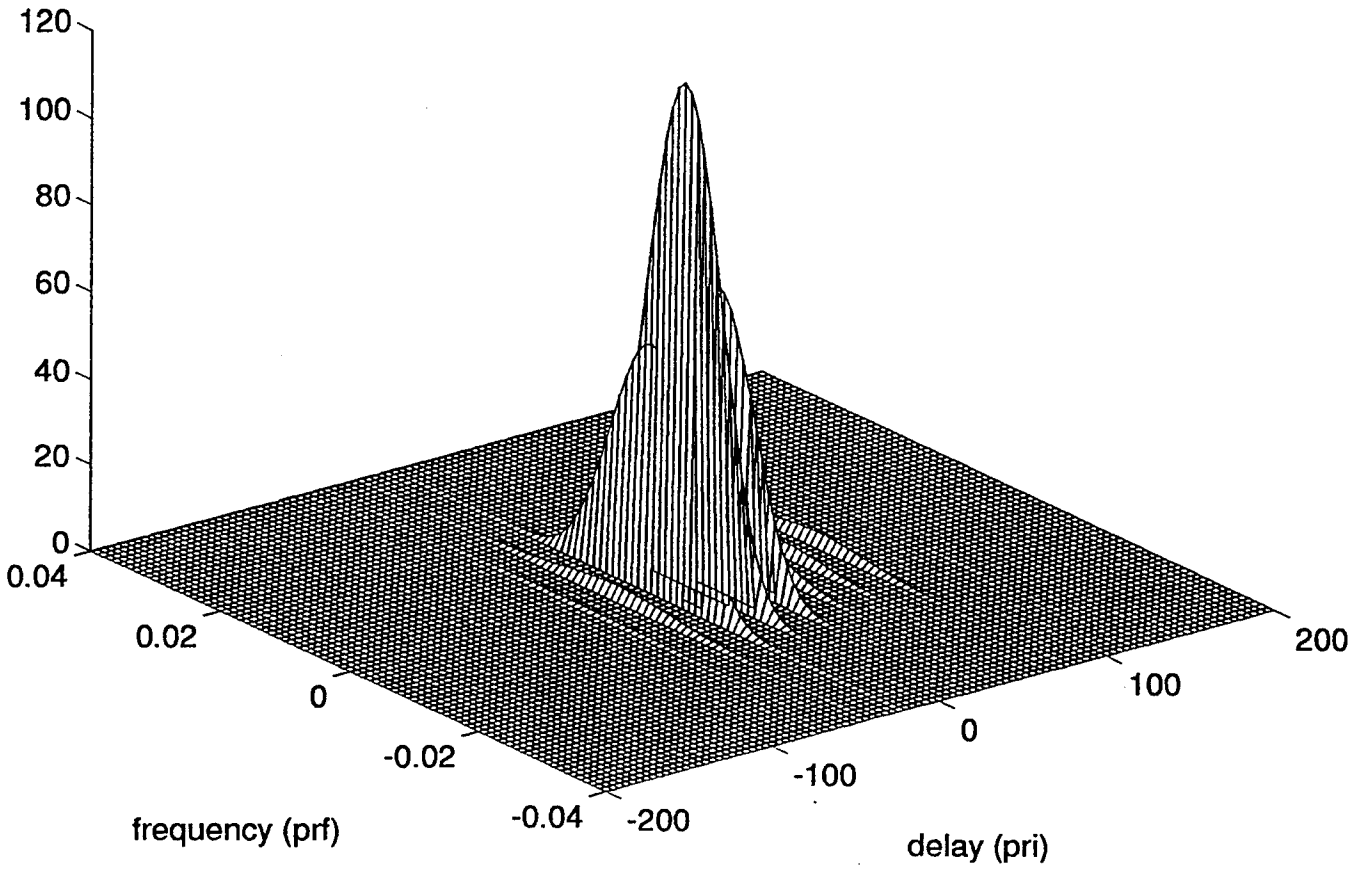

Figure 24. Cross-ambiguity Diagram of the Stepped Frequency Radar, Pulse Number N=150, Number of Pulses Processed M=100, Duty-cycle=0.2 , Δf =0.1PRF, I=50, l=0, and with Hamming Window

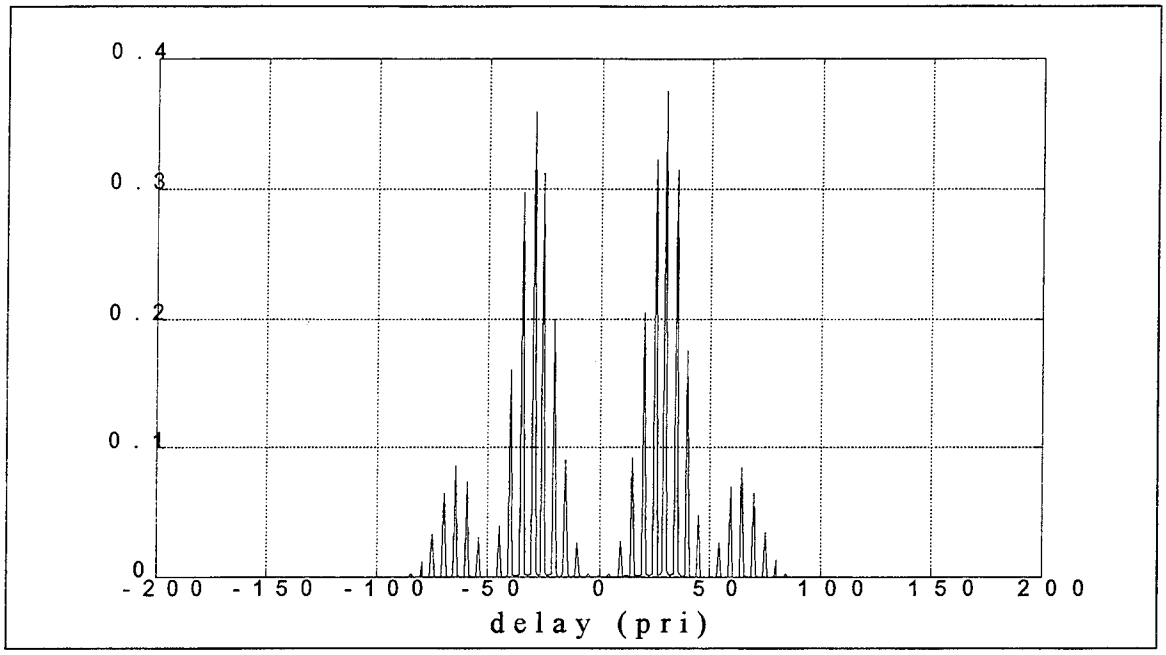

Figure 25. Plot of Cut Parallel to Time Axis for f=0.02PRF of the Cross-ambiguity Function for the Stepped Frequency Radar, Pulse Number N=100, Number of Pulses Processed M=100, Duty-cycle=0.2 , Δf =0.1PRF, I=0, l=0, and with Hamming Window

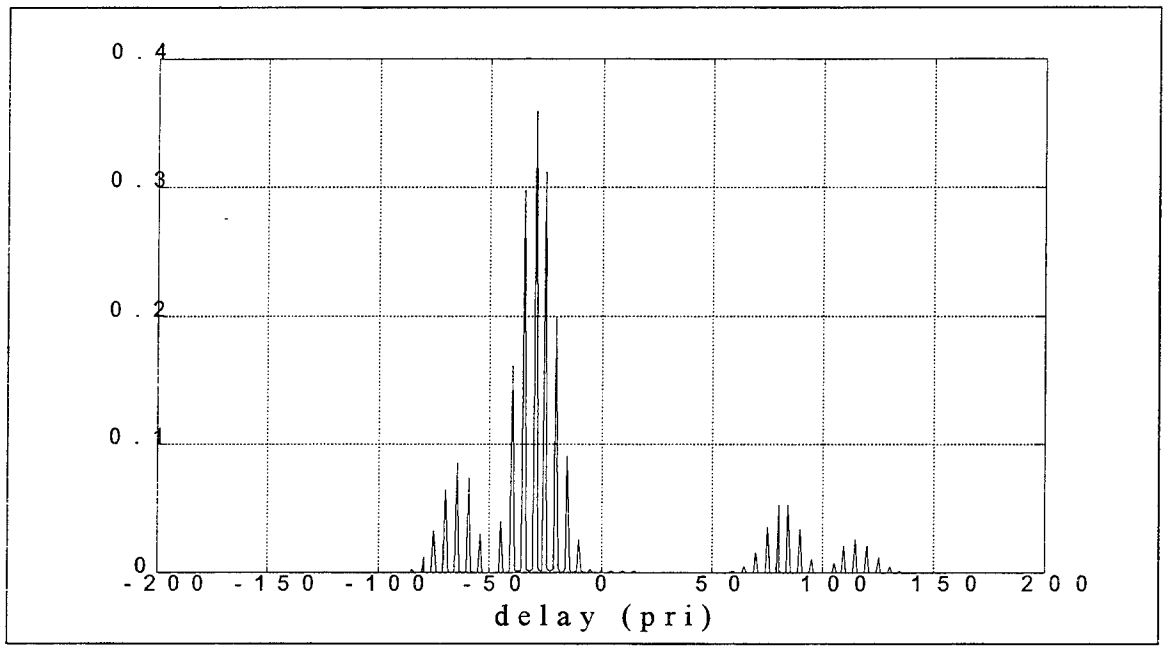

Figure 26. Plot of Cut Parallel to Time Axis for f=0.02PRF of the Cross-ambiguity Function for the Stepped Frequency Radar, Pulse Number N=150, Number of Pulses Processed M=100, Duty-cycle=0.2 ,Δf =0.1PRF, I=50, l=0, and with Hamming Window.

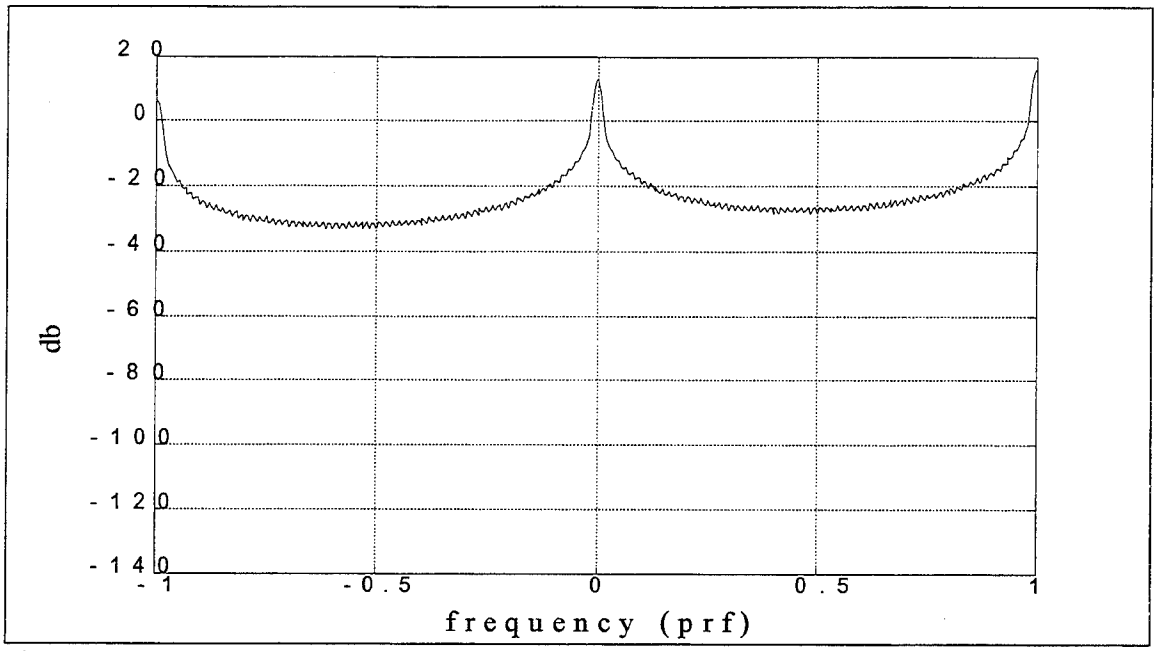

Figure 27. Plot of Cut Parallel to Frequency Axis for τ=30PRI of the Cross-ambiguity Function for the Stepped Frequency Radar, Pulse Number N=100, Number of Pulses Processed M=100, Duty-cycle=0.2 , Δf =0.1PRF, I=0, l=0, and with Hamming Window.

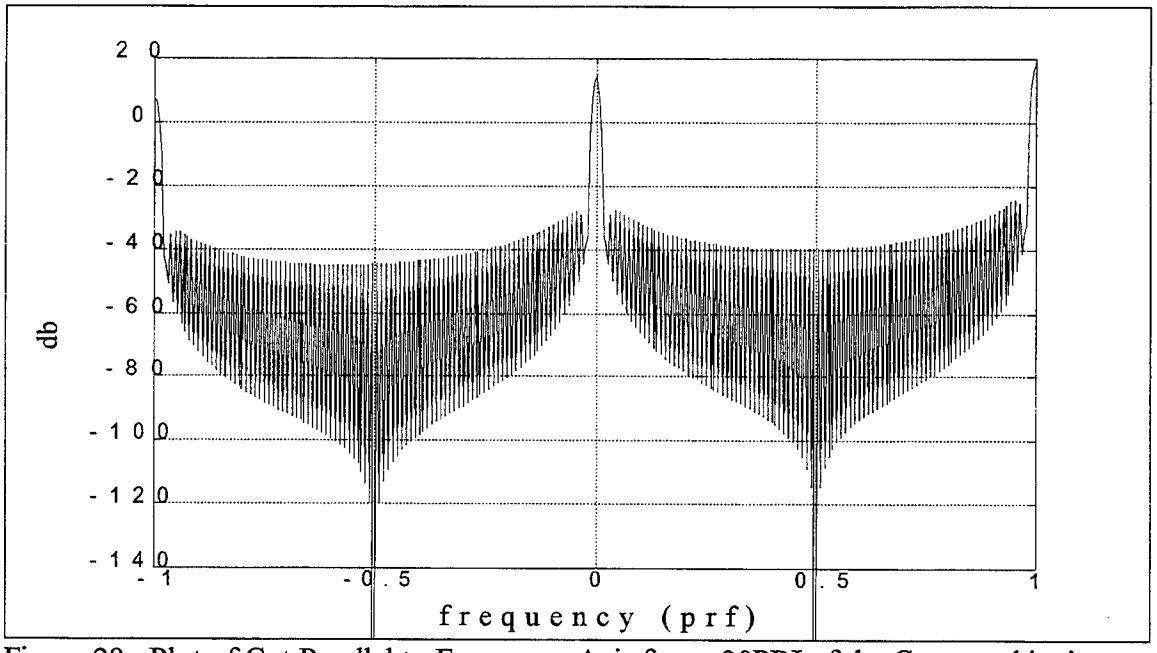

Figure 28. Plot of Cut Parallel to Frequency Axis for τ=30PRI of the Cross-ambiguity Function for the Stepped Frequency Radar, Pulse Number N=150, Number of Pulses Processed M=100, Duty-cycle=0.2, Δf =0.1PRF, I=50, l=0, and with Hamming Window.

IV. CONCLUSIONS

This thesis investigates the ambiguity functions of the stepped frequency waveform and the stepped frequency radar system. The stepped frequency waveform achieves a high range resolution by coherently processing the returns from N pulses, each having a different carrier frequency that changes by a fixed amount from pulse to pulse. The mathematical expression of the auto-ambiguity function for the stepped frequency waveform is derived from the definition. The auto-ambiguity function is defined as the correlation of the complex envelope of the transmitted signal and the Doppler frequency shifted version of the complex conjugate of the transmitted signal. The 3D plot of the auto-ambiguity function shown in Figure 5 is spiky like that of a constant frequency pulse train (shown in Figure A.5) and is tilted at an angle. Along the time delay axis, the null-to-null width of each spike is $2/N\Delta f$ as compared to $2/\tau$ for the constant frequency pulse train, thereby making it possible to decrease the width by increasing $N\Delta f$ without increasing its instantaneous bandwidth. However, for the constant frequency pulse train, high resolution can be achieved by decreasing the pulse width and, thereby, increasing the instantaneous bandwidth. On the other hand, the null-to-null spike width of the stepped frequency waveform along the frequency axis is equal to 2/(N×PRI) which is the same as for the constant frequency pulse train. Thus frequency resolution is not improved by the stepped frequency waveform.

The mathematical expression of the cross-ambiguity function for the high PRF stepped frequency radar system including its receiver and signal processor is also derived. This mathematical expression is obtained from the output of the Doppler processor and a distinct ambiguity function is defined for each Doppler processing filter. If weighting is ignored, the cross-ambiguity function of the 0th Doppler filter reduces to the auto-ambiguity function of the stepped frequency waveform derived from the traditional definition. Ambiguity functions of other Doppler filters are shifted versions of the auto-ambiguity function along the frequency axis. The mathematical expression has been verified by comparing the ambiguity diagram obtained by simulation which performs the correlation method.

The improvement of the clutter suppression capability for the stepped frequency radar system by rejecting initial pulses is also proven. The strong clutter returns from close range can be suppressed by rejecting some initial pulses, thereby reducing the interference from the region. Four types of basic waveforms are also discussed in the appendix for the purpose of comparison. These are single pulse, periodic constant frequency pulse train, linear frequency modulated pulse, and discrete frequency modulated pulse. The mathematical expressions of ambiguity functions for these waveforms are derived and have been also verified by simulation.

APPENDIX A. EXAMPLES OF THE AMBIGUITY FUNCTION FOR THE BASIC WAVEFORMS

In this section the ambiguity functions of commonly used radar signals such as single pulse, constant frequency pulse train, linear frequency modulated pulse, and discrete frequency modulated pulse are discussed. The mathematical expression of the ambiguity function for these waveforms are derived and verified by comparing with the ambiguity diagram obtained from the simulation.

1. Single Pulse of the Sine Wave

The single pulse of the sine wave can be defined as

$$S_t(t) = u(t)e^{j2\pi f_0 t} \ , \tag{A.1}$$

where $u(t)$ is the complex envelope of the signal, it is defined as

$$\begin{aligned} u(t) &= 1, \quad \text{if } 0 \le t < T_s \ , \\ &= 0, \quad \text{elsewhere, and} \end{aligned} \tag{A.2}$$

T_s is the pulse width.

The ambiguity function of the single pulse can be expressed as

$$\begin{aligned} X(\tau, f_d) &= \int_{-\infty}^{\infty} u(t-\tau)u^*(t)e^{j2\pi f_d t}dt \\ &= \int_{\tau}^{T_s} e^{j2\pi f_d t}dt \\ &= (T_s - \tau) \times e^{j\pi f_d (T_s+\tau)} \times \frac{\sin \pi f_d (T_s-\tau)}{\pi f_d (T_s-\tau)} , \quad \text{for } 0 \le \tau < T_s, \end{aligned} \tag{A.3-1}$$

$$X(\tau, f_d) = (T_s + \tau) \times e^{j\pi f_d (T_s+\tau)} \times \frac{\sin \pi f_d (T_s+\tau)}{\pi f_d (T_s+\tau)} , \quad \text{for } -T_s < \tau < 0, \tag{A.3-2}$$

$$X(\tau, f_d) = 0, \quad \text{elsewhere.} \tag{A.3-3}$$

The absolute value of the ambiguity function of the single pulse can be expressed as

$$|X(\tau,f_d)| = (T_s-\tau)\times\left|\frac{\sin\pi f_d(T_s-\tau)}{\pi f_d(T_s-\tau)}\right| , \quad \text{for } 0\le\tau<T_s, \tag{A4-1}$$

$$|X(\tau,f_d)| = (T_s+\tau)\times\left|\frac{\sin\pi f_d(T_s+\tau)}{\pi f_d(T_s+\tau)}\right|, \quad \text{for } -T_s<\tau<0, \tag{A4-2}$$

$$|X(\tau,f_d)| = 0, \qquad \text{elsewhere.} \tag{A4-3}$$

The ambiguity function along the Doppler frequency shift axis, τ=0, becomes

$$|X(0,f_d)| = T_s\times\left|\frac{\sin(\pi f_d T_s)}{\pi f_d T_s}\right| \tag{A.5}$$

The ambiguity function along the time delay axis, f_d=0, becomes

$$|X(\tau,0)| = T_s-\tau , \qquad \text{for } 0\le\tau<T_s, \tag{A.6-1}$$

$$= T_s+\tau , \qquad \text{for } -T_s<\tau<0, \tag{A.6-2}$$

$$= 0, \qquad \text{elsewhere.} \tag{A.6-3}$$

The ambiguity diagram, $|X(\tau,f_d)|^2$, of the single pulse is shown in Figure A.1, the contour plot is shown in Figure A.2, and plots of cut along the frequency axis for τ=0 and time delay axis for f_d=0 are shown in Figure A.3 and Figure A.4. The plot for zero time delay is the square of the spectrum of a rectangular pulse which is the square of the absolute value of the SINC function. The plot for zero frequency shift represents the magnitude square of the auto-correlation function of a rectangular pulse.

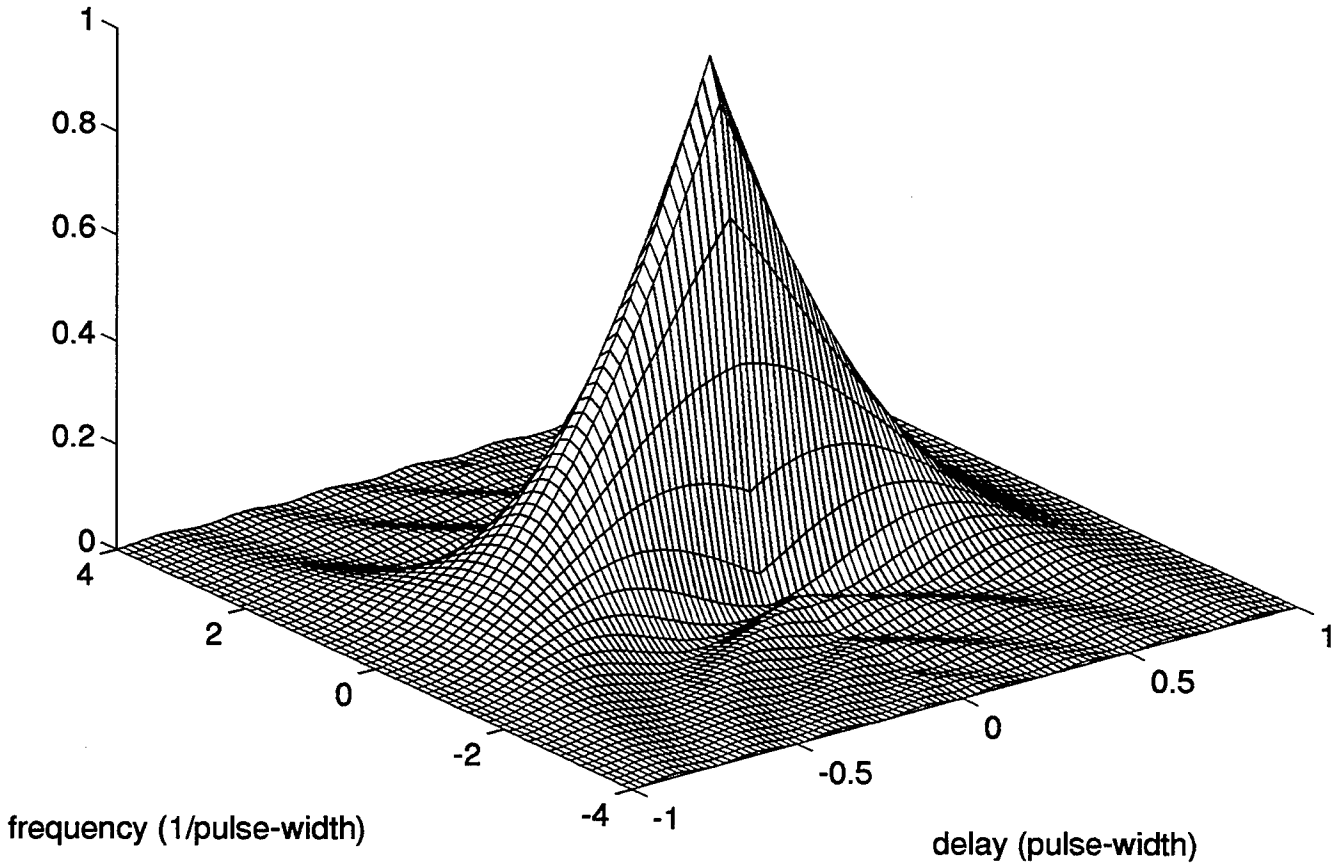

Figure A.1. Ambiguity Diagram of A Single Pulse, Pulse Width=1.

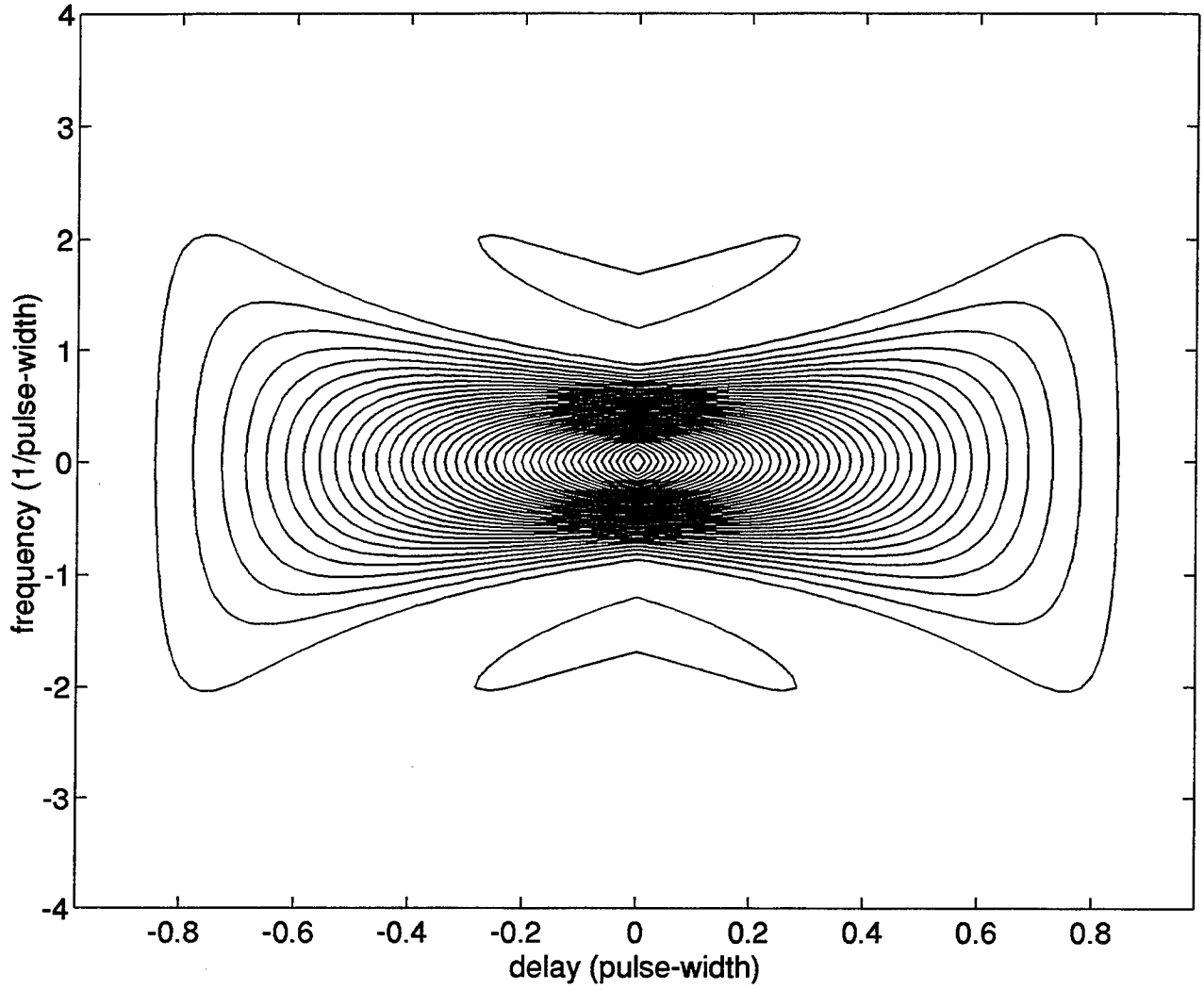

Figure A.2. Contour Plot of the Ambiguity Diagram of A Single Pulse, Pulse Width=1.

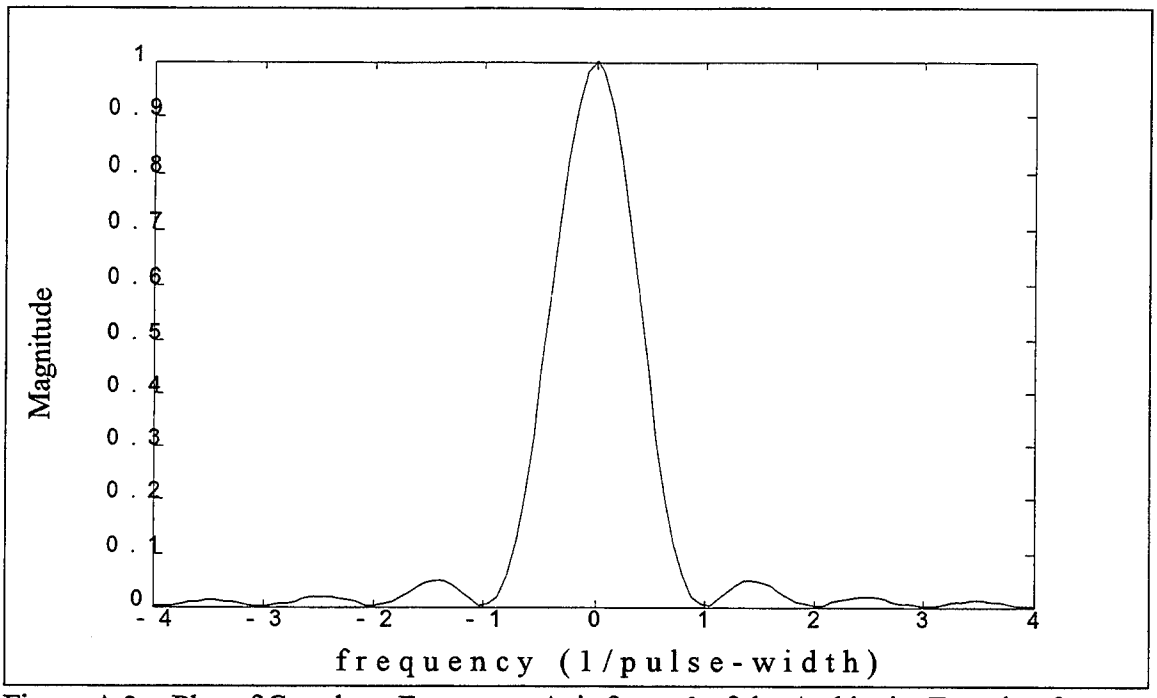

Figure A.3. Plot of Cut along Frequency Axis for τ=0 of the Ambiguity Function for A Single Pulse, Pulse Width=1.

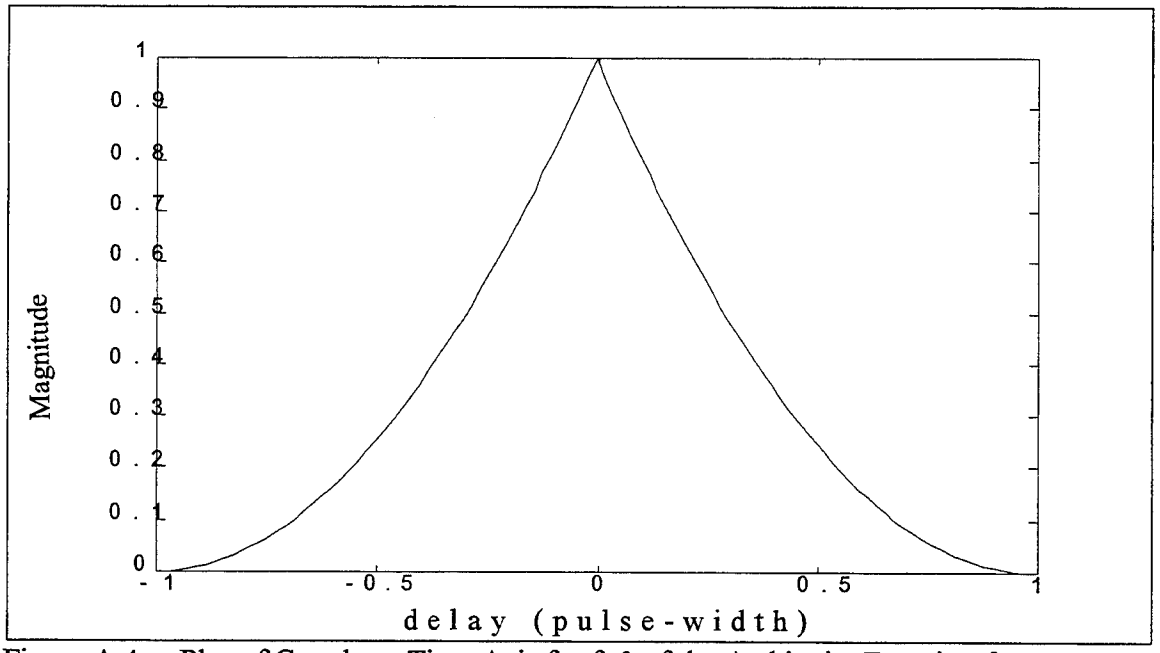

Figure A.4. Plot of Cut along Time Axis for f=0 of the Ambiguity Function for A Single Pulse, Pulse Width=1.

2. Constant Frequency Pulse Train

Constant frequency pulse train of N pulses can be defined as

$$S_t(t) = \sum_{n=0}^{N-1} \mu(t - nT_r) e^{j2\pi f_0 t}, \tag{A.7}$$

where $\mu(t)$, the complex envelope of the single pulse of transmitted signal, is defined as

$$\begin{aligned} \mu(t - nT_r) &= 1, && \text{if } nT_r \le t < nT_r + T_s, \\ &= 0, && \text{elsewhere}, \end{aligned} \tag{A.8}$$

where

N : the number of pulses,
T_r : pulse repetition interval (PRI),
f_0 : carrier frequency.

The ambiguity function of periodic pulse train can be derived as

$$X(\tau, f_d) = \int_{-\infty}^{\infty} \sum_{n=0}^{N-1} \mu(t - nT_r - \tau) \sum_{m=0}^{N-1} \mu^*(t - mT_r) e^{j2\pi f_d t} dt \tag{A.9}$$

After changing variable, we obtain the ambiguity function as

$$X(\tau, f_d) = \sum_{n=0}^{N-1} \sum_{m=0}^{N-1} e^{j2\pi f_d n T_r} \int_{-\infty}^{\infty} \mu(t) \mu^*(t - (m-n)T_r - \tau) e^{j2\pi f_d t} dt \tag{A.10}$$

Now we define the round trip time in terms of integer and fraction parts

$$\tau = (p + \gamma) T_r \tag{A.11}$$

where p is integer ,γ is the fraction, and $0 \le \gamma < 1$.

After substituting Equation A.11 in Equation A.10 and simplifying , we obtain the expression for the ambiguity function as

$$X(\tau,f_d) = (T_s-\gamma T_r)\times e^{j\pi f_d(T_s+\gamma T_r)}\times\frac{\sin\pi f_d(T_s-\gamma T_r)}{\pi f_d(T_s-\gamma T_r)}\times\sum_{n=\max(0,p)}^{\min(N-1,N-1+p)} e^{j2\pi f_d nT_r},$$

$$\text{for } 0\le\gamma<\frac{T_s}{T_r}, \qquad \text{(A.12-1)}$$

$$=(T_s+(\gamma-1)T_r)\times e^{j\pi f_d(T_s+(\gamma-1)T_r)}\times\frac{\sin\pi f_d(T_s+(\gamma-1)T_r)}{\pi f_d(T_s+(\gamma-1)T_r)}\times\sum_{n=\max(0,p+1)}^{\min(N-1,N+p)} e^{j2\pi f_d nT_r},$$

$$\text{for } 1-\frac{T_s}{T_r}\le\gamma<1, \qquad \text{(A.12-2)}$$

$$=0, \qquad \text{elsewhere.} \qquad \text{(A.12-3)}$$

We can now obtain the ambiguity function as the following equation after simplifying the summation term and taking the absolute value.

$$|X(\tau,f_d)| = (T_s-\gamma T_r)\times\left|\frac{\sin\pi f_d(T_s-\gamma T_r)}{\pi f_d(T_s-\gamma T_r)}\right|\times\left|\frac{\sin\pi f_d(N-|p|)T_r}{\sin\pi f_d T_r}\right|,$$

$$\text{for } 0\le\gamma<\frac{T_s}{T_r}, \qquad \text{(A13-1)}$$

$$|X(\tau,f_d)| = (T_s+(\gamma-1)T_r)\times\left|\frac{\sin\pi f_d(T_s+(\gamma-1)T_r)}{\pi f_d(T_s+(\gamma-1)T_r)}\right|\times\left|\frac{\sin\pi f_d(N-|p+1|)T_r}{\sin\pi f_d T_r}\right|,$$

$$\text{for } 1-\frac{T_s}{T_r}\le\gamma<1, \qquad \text{(A13-2)}$$

$$|X(\tau,f_d)| = 0, \qquad \text{elsewhere.} \qquad \text{(A13-3)}$$

The ambiguity function along the frequency axis, i.e., $\tau = 0$, can be expressed as

$$|X(0,f_d)| = T_s \times |\frac{\sin(\pi f_d T_s)}{\pi f_d T_s}| \times |\frac{\sin(\pi N f_d T_r)}{\sin(\pi f_d T_r)}| . \qquad \text{(A.14)}$$

The ambiguity function along the time delay axis, i.e., $f_d = 0$, is expressed as

$$|X(\tau,0)| = (N - |p|)(T_s - \gamma T_r), \quad \text{for } 0 \le \gamma < \frac{T_s}{T_r}, \qquad \text{(A.15-1)}$$

$$= (N - |p+1|)((\gamma - 1)T_r + T_s), \quad \text{for } 1 - \frac{T_s}{T_r} \le \gamma < 1, \qquad \text{(A.15-2)}$$

$$= 0, \quad \text{elsewhere.} \qquad \text{(A.15-3)}$$

The ambiguity diagram of the pulse radar according to Equation A.13 is shown in Figure A.5 and the contour of the ambiguity diagram is shown in Figure A.6. Plots of cut along frequency axis for τ=0 and cut along time delay axis for f_d=0 are shown in Figure A.7 and A.8. From Equation A.14 and Figure A.7, spikes appear at frequencies which are multiples of PRF. The first null for each spike is $1/NT_r$ away from the center of the spike. Therefore, each spike has the null to null width of $2/NT_r$ in the frequency axis. Amplitudes of those spikes varies as a SINC function. Zero amplitude will appear at $1/T_s$. From Equation A.15 and Figure A.8, it is seen that there are 2N-1 spikes along the time delay axis each of which has the width of $2T_s$. The plot of cut of the ambiguity function at zero frequency shift represents the magnitude square of the auto-correlation function of a pulse train.

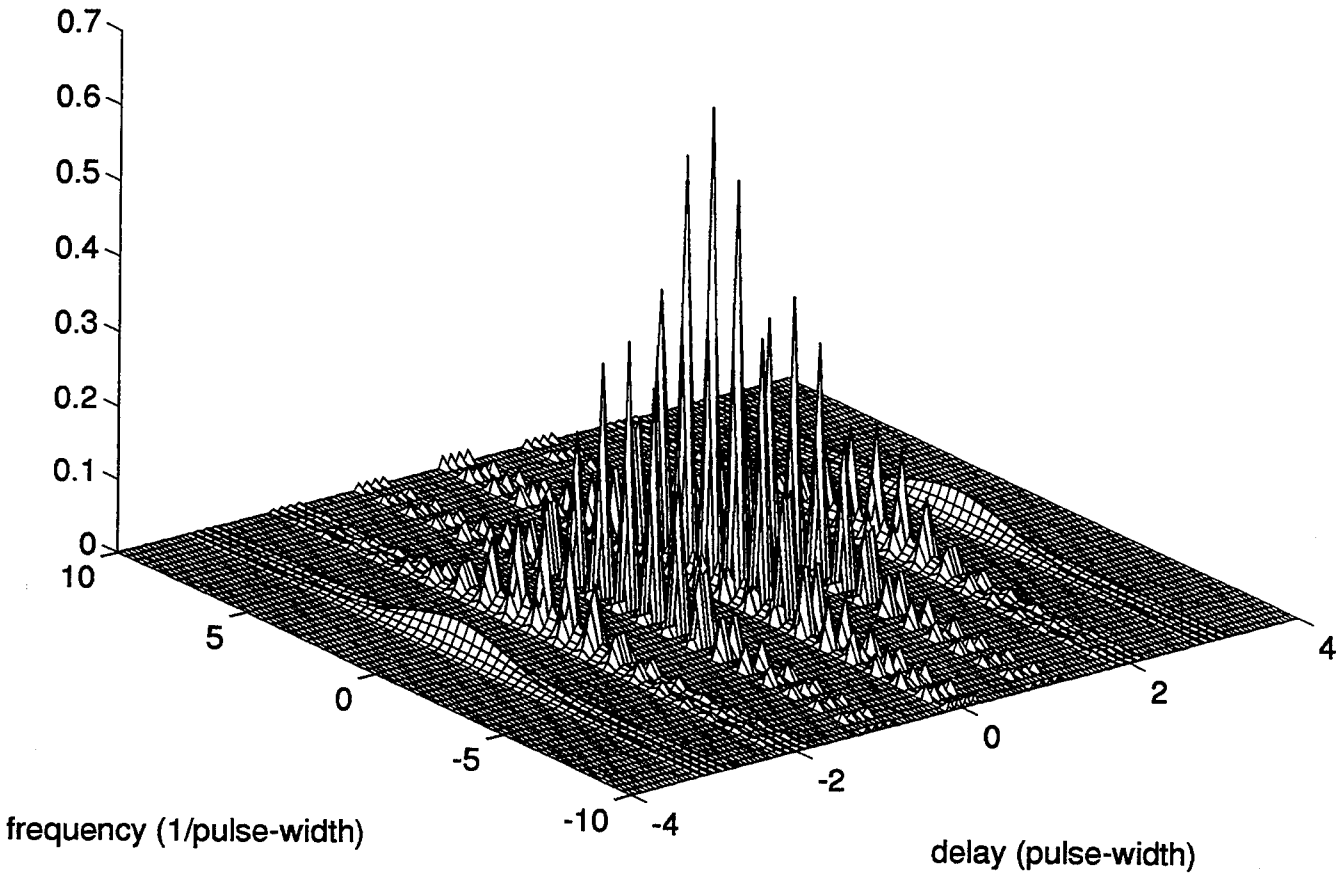

Figure A.5. Ambiguity Diagram of the Pulse Radar, Number of Pulses N=4, Duty-cycle=0.2.

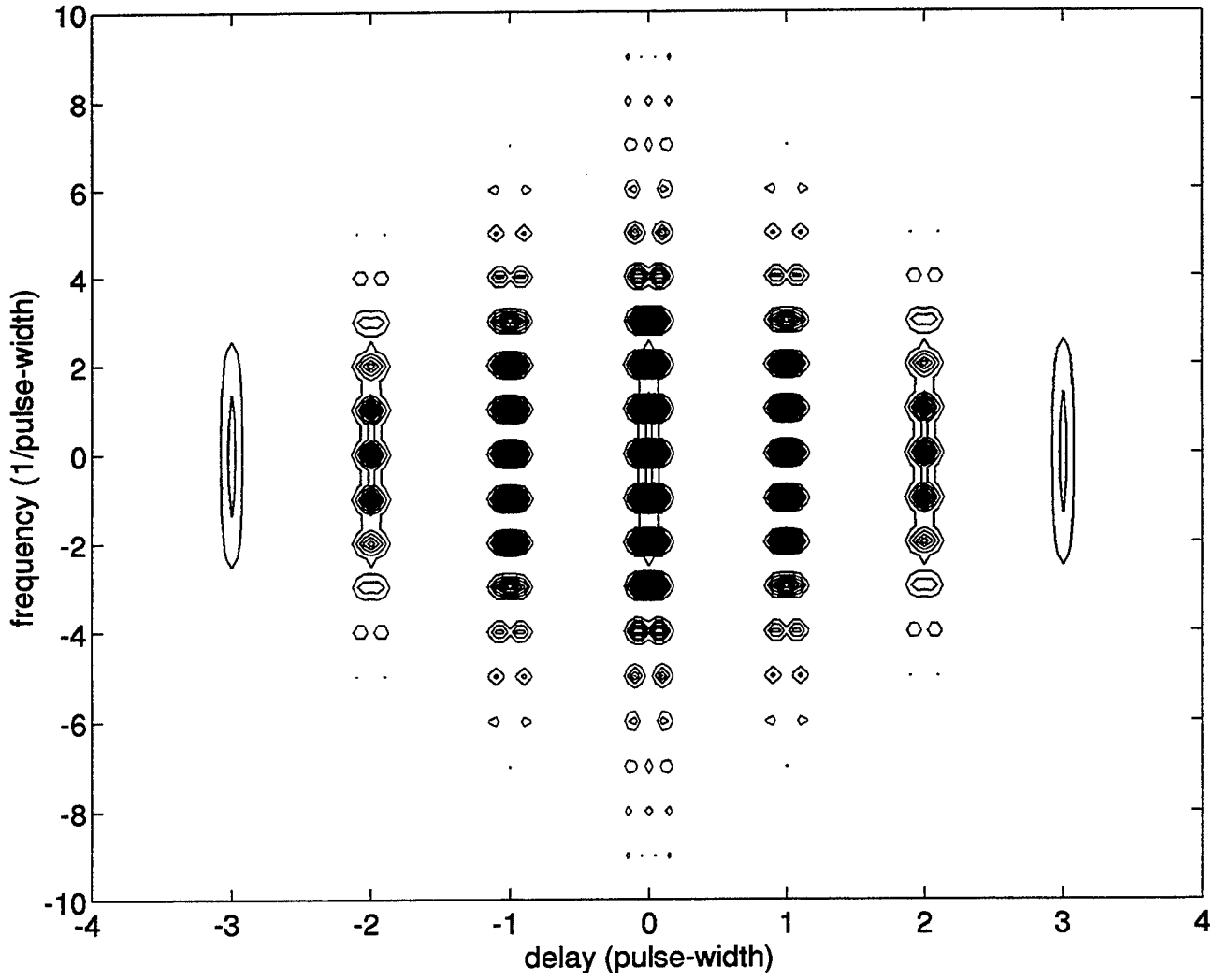

Figure A.6. Contour Plot of the Ambiguity Diagram for the Pulse Radar, Number of Pulses N=4, Duty-cycle=0.2.

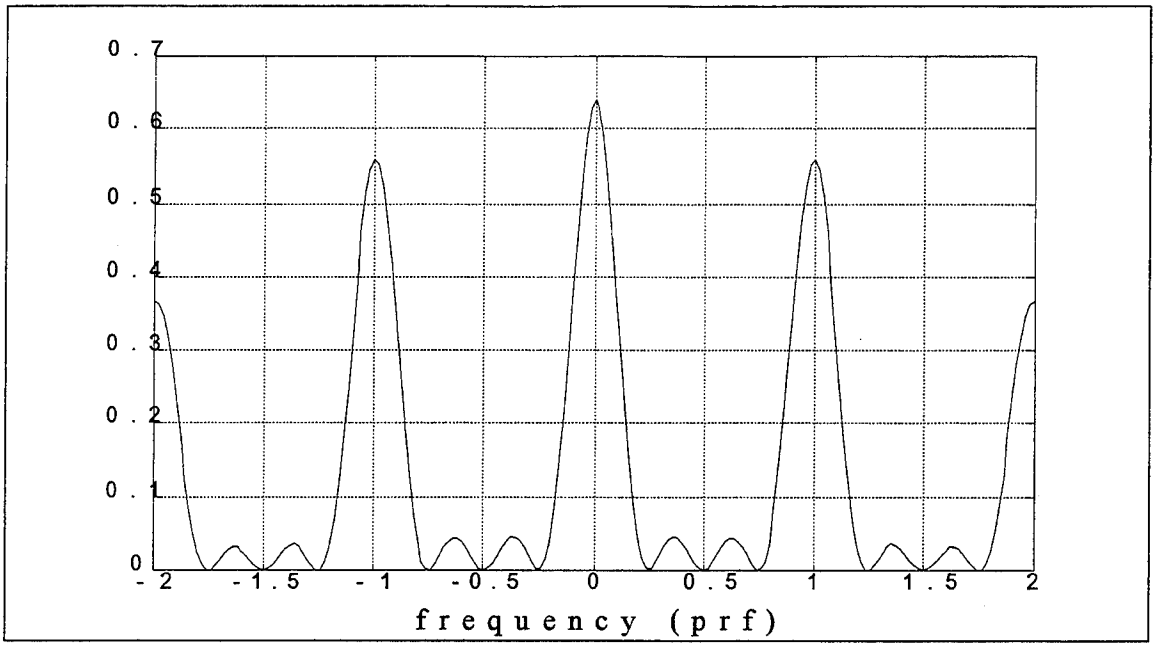

Figure A.7. Plot of Cut along Frequency Axis for τ=0 of the Ambiguity Function for the Pulse Radar, Number of Pulses N=4, Duty-cycle=0.2.

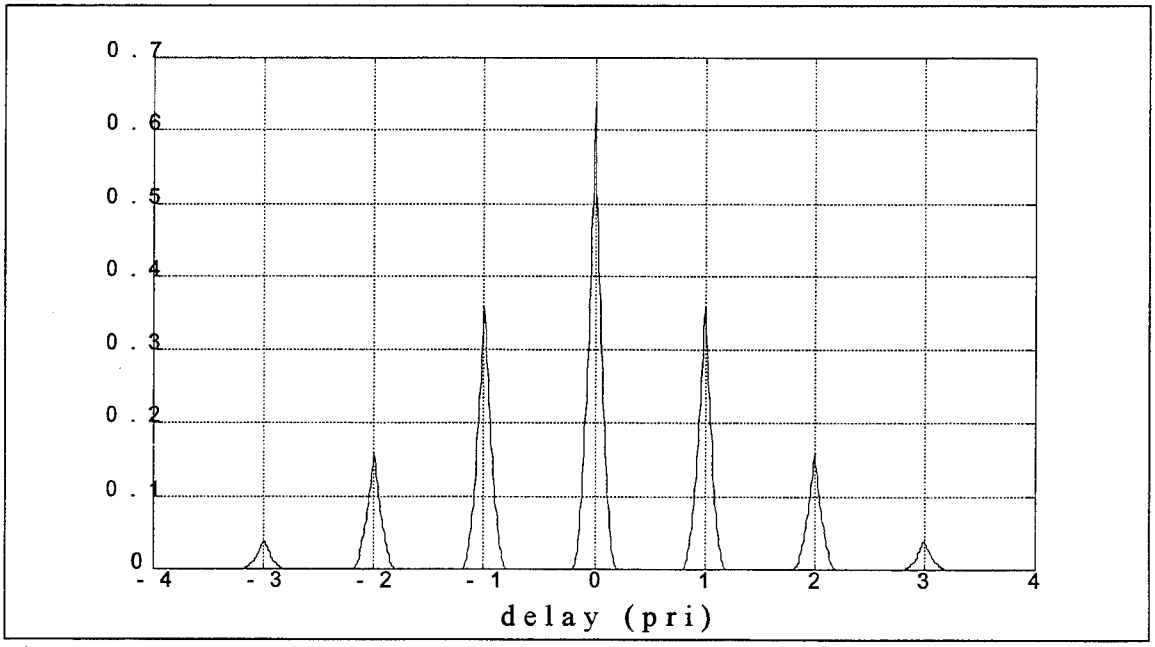

Figure A.8. Plot of Cut along Time Axis for f=0 of the Ambiguity Function for the Pulse Radar, Number of Pulses N=4, Duty-cycle=0.2.

3. Linear Frequency Modulated Pulse

Linear frequency modulated pulse can be mathematically represented as

$$S_t(t) = u(t)e^{j2\pi\left(f_0 t+\frac{1}{2}\mu t^2\right)}$$

$$= \left[u(t)e^{j\pi\mu t^2}\right]e^{j2\pi f_0 t}, \qquad \text{(A.16)}$$

where $u(t)$ was defined in Equation A.2 and μ is the rate of frequency change. The ambiguity function of the linear frequency modulated pulse can be written as

$$X(\tau, f_d) = \int_{-\infty}^{\infty} u(t-\tau)e^{j\pi\mu(t-\tau)^2}u^*(t)e^{-j\pi\mu t^2}e^{j2\pi f_d t}dt$$

$$= \int_{-\infty}^{\infty} u(t-\tau)u^*(t)e^{j2\pi(f_d-\mu\tau)t}dt. \qquad \text{(A.17)}$$

Equation A.17 is exactly the same as Equation A.3, except that f_d is replaced by f_d-$\mu\tau$. The ambiguity function becomes

$$|X(\tau, f_d)| = (T_s-\tau)\times\left|\frac{\sin\pi(f_d-\mu\tau)(T_s-\tau)}{\pi(f_d-\mu\tau)(T_s-\tau)}\right|, \quad \text{for } 0\le\tau<T_s, \qquad \text{(A.18-1)}$$

$$= (T_s+\tau)\times\left|\frac{\sin\pi(f_d-\mu\tau)(T_s+\tau)}{\pi(f_d-\mu\tau)(T_s+\tau)}\right|, \quad \text{for } -T_s<\tau<0, \qquad \text{(A.18-2)}$$

$$= 0, \quad \text{elsewhere.} \qquad \text{(A.18-3)}$$

The ambiguity diagram is shown in Figure A.9 and contour plot is shown in Figure A.10. From Figure A.2 and Figure A.10, it can be seen that the ambiguity function of the LFM pulse is a rotated version of the ambiguity function of a single pulse. The angle of rotation depends upon the rate of frequency change μ as shown in Figure A.11.

4. Discrete Frequency modulated Pulse

The discrete frequency modulated pulse consists of N subpulses, each at different discrete carrier frequency. Such a pulse can be expressed as

$$S_t(t) = \sum_{n=0}^{N-1} u(t-nT)e^{j2\pi(f_0+n\Delta f)t}, \qquad \text{(A.19)}$$

where N is the number of the discrete frequencies in the pulse, NT is the pulse width, and u(t) is defined as

$$\begin{aligned} u(t-nT) &= 1, \quad && \text{if } nT \le t < (n+1)T, \\ &= 0, && \text{elsewhere.} \end{aligned} \qquad \text{(A.20)}$$

The envelope of the transmitted signal can be written as

$$U(t) = \sum_{n=0}^{N-1} u(t-nT)e^{j2\pi n\Delta ft}. \qquad \text{(A.21)}$$

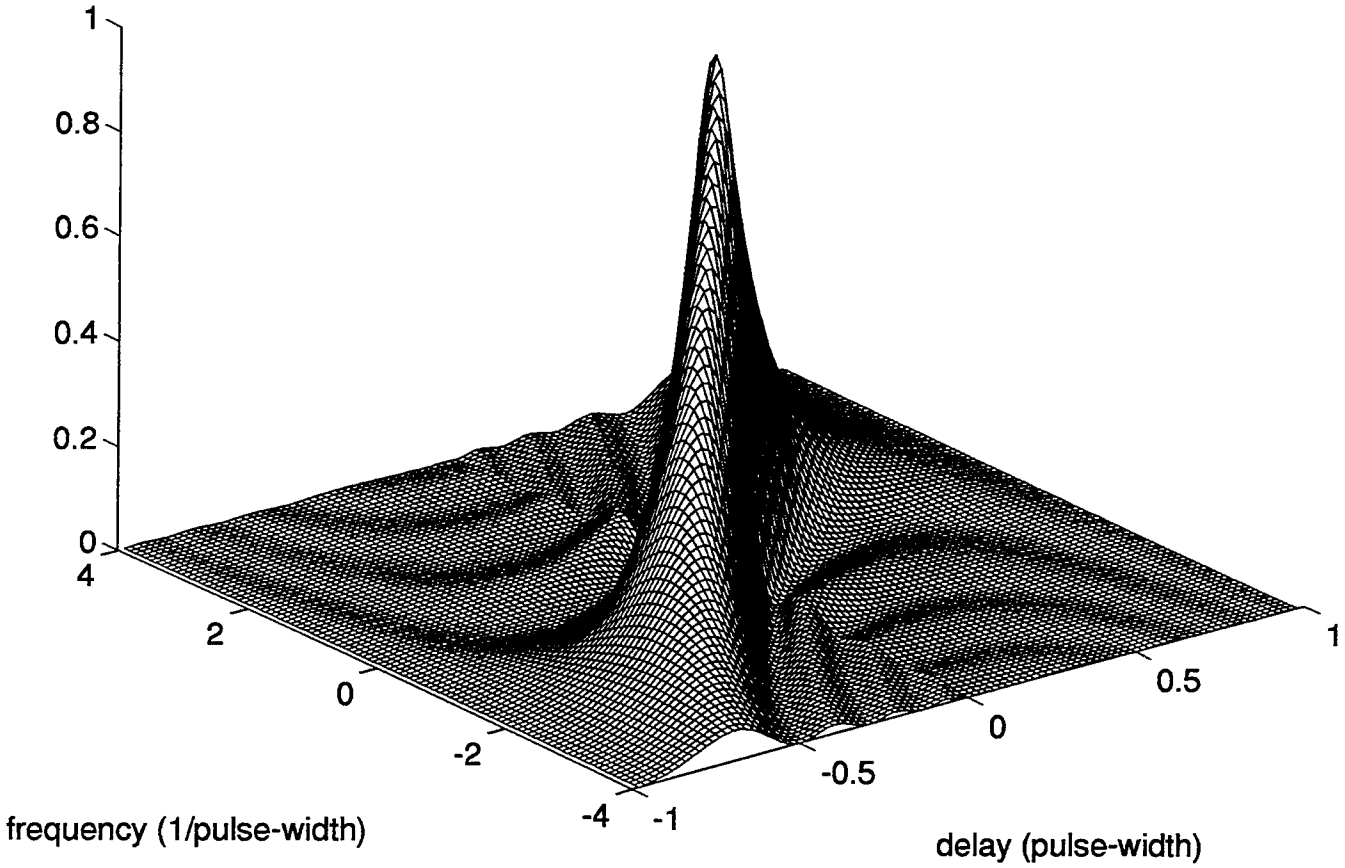

Figure A.9. Ambiguity Diagram of the LFM Pulse, Pulse Width=1.

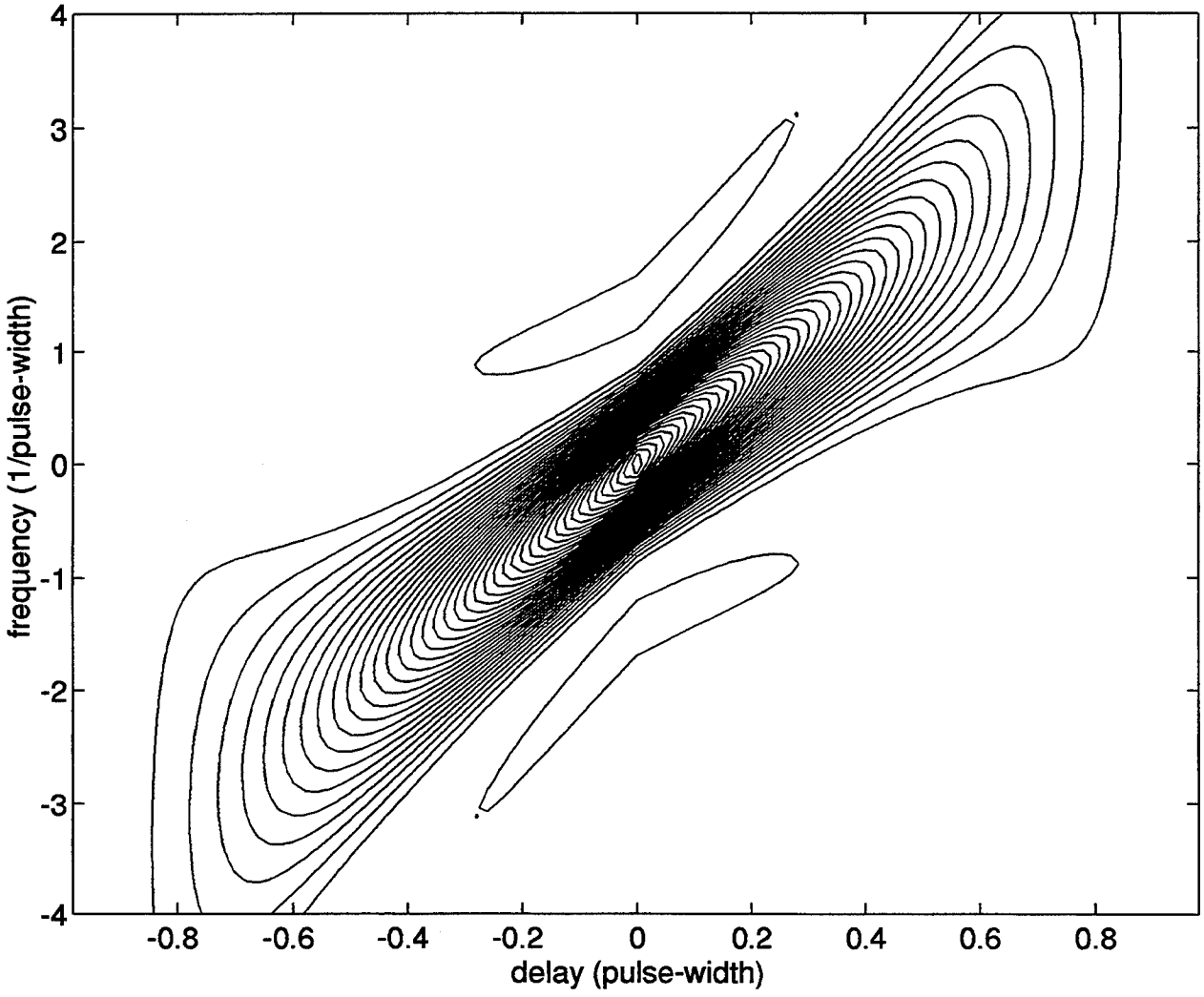

Figure A.10. Contour Plot of the Ambiguity Diagram of the LFM Pulse, Pulse Width=1.

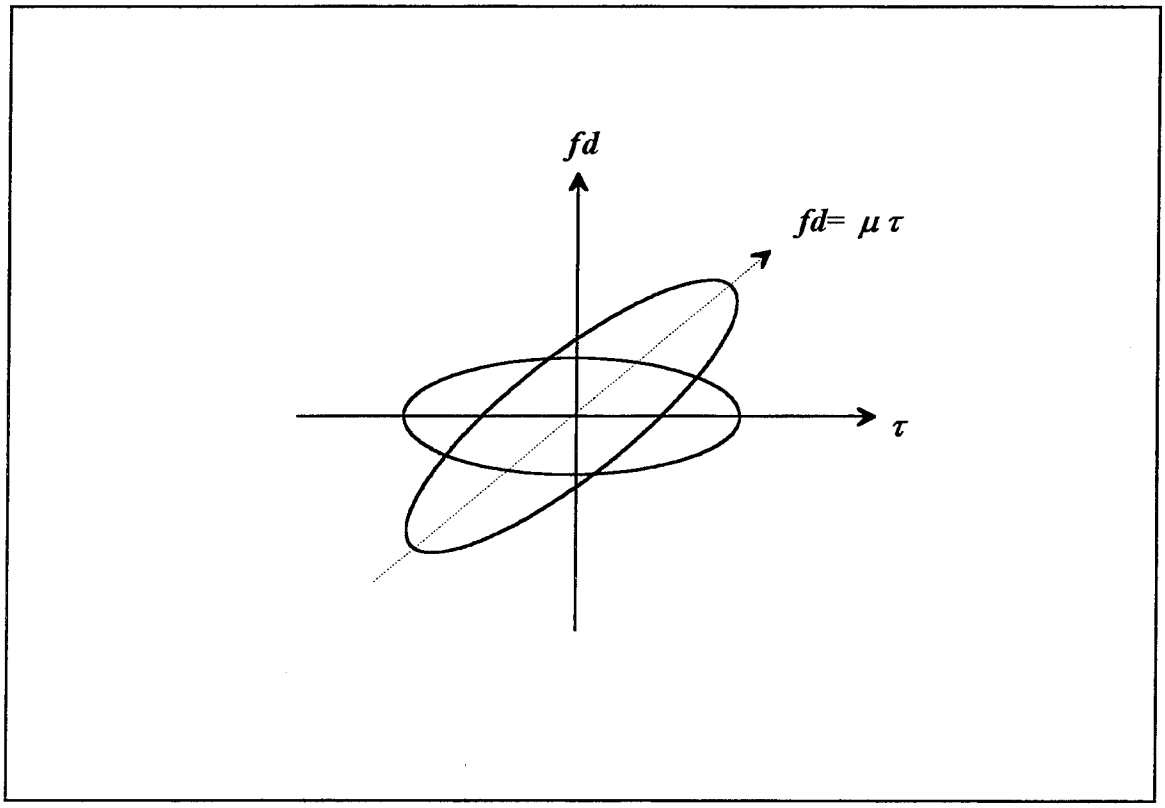

Figure A.11. The Relation of the Ambiguity Functions for the Single Pulse and LFM Pulse.

According to the definition of the ambiguity function, we obtain the ambiguity function of the discrete frequency modulated pulse as

$$X(\tau,f_d)=\int_{-\infty}^{\infty} U(t-\tau)U^*(t)e^{j2\pi f_d t}dt. \tag{A.22}$$

Now we define the round trip time in terms of integer and fraction parts,

$$\tau=(p+\gamma)T, \tag{A.23}$$

where p is an integer and γ is a fraction where $0\le\gamma<1$. We can obtain the ambiguity function of the discrete frequency modulated pulse after simplification. The expression of the ambiguity function has the form as

$$X(\tau,f_d)=\{(1-\gamma)T\times e^{j\pi(f_d-p\Delta f)(1+\gamma)T}\times e^{j2\pi p\Delta f\tau}\times e^{j\pi(f_d-(2p+\gamma)\Delta f)(N-1+p)T}\times$$

$$\frac{\sin\pi(f_d-p\Delta f)(1-\gamma)T}{\pi(f_d-p\Delta f)(1-\gamma)T}\times\frac{\sin\pi(f_d-(2p+\gamma)\Delta f)(N-|p|)T}{\sin\pi(f_d-(2p+\gamma)\Delta f)T}\}+$$

$$\{\gamma T\times e^{j\pi(f_d-(p+1)\Delta f)\gamma T}\times j2\pi(p+1)\Delta f\tau\times e^{j\pi(f_d-(2p+\gamma+1)\Delta f)(N+p)T}\times$$

$$\frac{\sin\pi(f_d-(p+1)\Delta f)\gamma T}{\pi(f_d-(p+1)\Delta f)\gamma T}\times\frac{\sin\pi(f_d-(2p+\gamma+1)\Delta f)(N-|p+1|)T}{\sin\pi(f_d-(2p+\gamma+1)\Delta f)T}\}. \tag{A.24}$$

The ambiguity diagram is shown in Figure A.12 and contour plot is shown in Figure A.13. The discrete frequency modulated pulse is composed of the linear frequency modulated signal and the pulse train with 100% duty-cycle. Therefore, the ambiguity diagram of it has been tilted and has many discrete spikes.

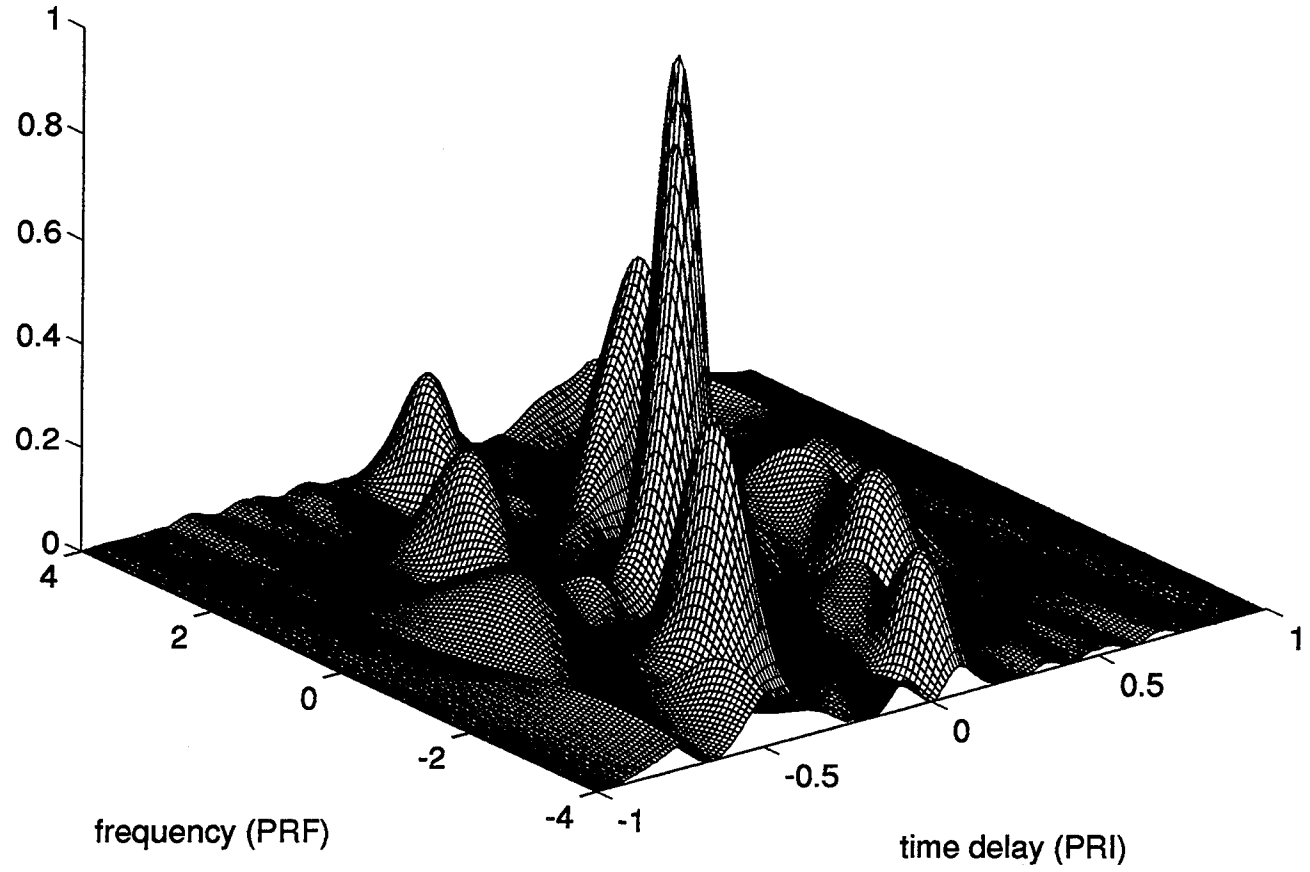

Figure A.12. Ambiguity Diagram of the Discrete FM Pulse, Pulse Width=1.

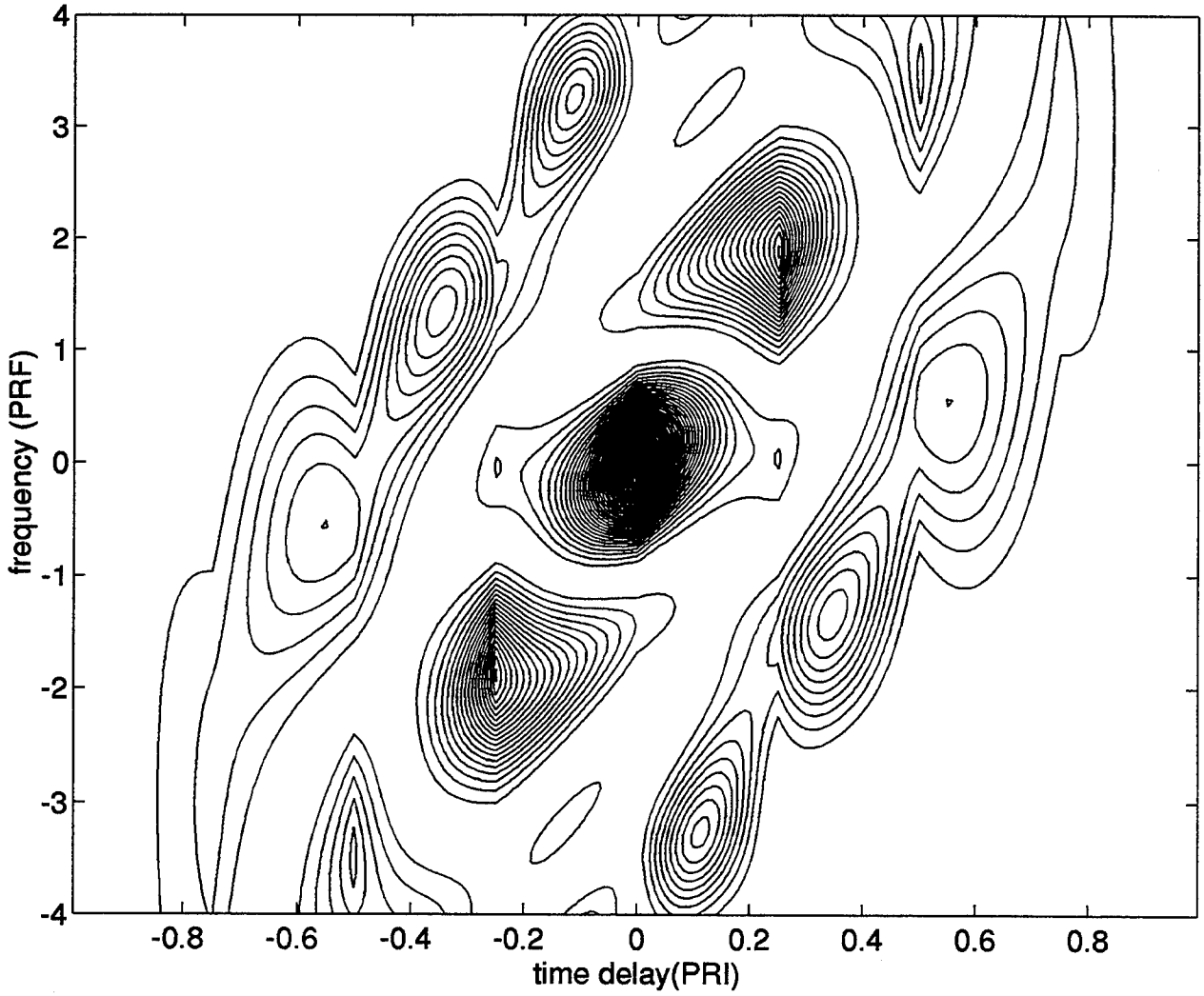

Figure A.13. Contour Plot of the Ambiguity Diagram of the Discrete FM Pulse, Pulse Width=1.

APPENDIX B. AMBIGUITY FUNCTION PROGRAM CODES

```
**************************************************************************

%filename : prog1.m
%Ambiguity function of the single pulse by correlation method
%update : 27/sep/94
%by : Huang, Jen-chih
%
clear;                                  %clear all the variable
tau=1;                                  %pulse width =1
nx=50;                                  %# of step in delay axis
ny=101;                                 %# of step in frequency axis
t=[0:nx-1]*tau/nx;                      %time axis
dt=t(2)-t(1);                           %time step
z=[];
fd=linspace(-4/tau,4/tau,ny)            %frequency axis
u1=ones(1,nx);                          %envelope of the transmitted signal
for m=1:ny
u2=u1.*exp(j*2*pi*fd(m)*t);             %u1 multiply by doppler freq. shift
c=xcorr(u2,u1).*dt;                     %correlation of u1 & u2
z=[z;(abs(c)).^2];                      %matrix of the ambiguity function
end
t=[fliplr(-t),t(2:nx)];                 %reconstruct the time axis
figure(1)
mesh(t,fd,z)
title('Ambiguity diagram of single pulse')
xlabel('delay (pulse-width)')
ylabel('frequency (1/pulse-width)')
figure(2)
plot(t,z((ny+1)/2,:))                   %plot of cut along frequency axis
xlabel('delay (pulse-width)')
ylabel('frequency (1/pulse-width)')
figure(3)
plot(fd,z(:,nx))                        %plot of cut along delay axis
xlabel('delay (pulse-width)')
ylabel('frequency (1/pulse-width)')

**************************************************************************
```

```
**************************************************************************
%filename : prog2.m
%Ambiguity function of the linear frequency modulation (LFM) pulse
%by correlation method
%update : 15/aug/94
%by : Huang, Jen-chih
%
%
clear;                          %clear all the variables
tau=1;                          %pulse width=1
mu=4;                           %rate of frequency change
nx=50;                          %# of step in delay axis
ny=101;                         %# of step in frequency axis
t=[0:nx-1]*tau/nx;              %time axis
dt=t(2)-t(1);                   %time step
z=[];
fd=linspace(-4/tau,4/tau,ny);   %frequency axis
for m=1:ny
u1=exp(j*pi*mu.*t.*t);          %envelope of the transmitted signal
u2=conj(u1).*exp(j*2*pi*fd(m)*t); %u1 multiply Doppler frequency shift
c=conv(u2,fliplr(u1)).*dt;      %correlation of u1 & u2
z=[z;(abs(c)).^2];              %matrix of the mag. square of the ambiguity function
end
%
t=[fliplr(-t),t(2:nx)];         %reconstruct the time axis
figure(1)
mesh(t,fd,z)                    %mesh plot of ambiguity function
title('Ambiguity function of the single pulse')
xlabel('delay (pulse-width)')
ylabel('frequency (1/pulse-width)')
figure(2)
contour(t,fd,z,40)              %contour plot of the ambiguity function
title('Contour plot of the signal pulse')
xlabel('delay (pulse-width)')
ylabel('frequency (1/pulse-width)')
%
**************************************************************************
```

```
**************************************************************************
%filename : prog3.m
%Ambiguity function of the stepped frequency radar by the correlation method
%update : 15/mar/94
%by : Huang, Jen-chih
%
clear;
tau=0.2;                          %pulse width
t0=0.8;                           %PRI-pulse-width;  PRI=1
df=0;                             %step frequency
%                                 % if df=0 then pulse radar
%                                 %else stepped frequency radar
fs=40;                            %sample rate (Hz)
N=4;                              %# of pulses
T=N*(tau+t0);                     %total time period for N pulses
sn=fs*tau;                        %# of samples in pulse width
tn=fs*t0;                         %# of samples between pulses
Tn=sn+tn;                         % of samples in one PRI
P=[ones(1,sn),zeros(1,tn)];       %envelope for one PRI
t=linspace(0,T,N*Tn);             %time axis for N pulses
nx=101;                           %# of samples in frequency axis
fd=linspace(-10,10,nx);           %frequency axis
dt=t(2)-t(1);                     %time step
s=[];
m=[1,2,3,4];                     %step frequency sequence
for n=1:N
s=[s,exp(j*2*pi*(m(n)-1)*df*t(Tn*(n-1)+1:Tn*n)).*P];  %transmitted signal
end
z=[];
for L=1:mx
f=fd(L);
s1=conj(s).*exp(j*2*pi*f*t);      %transmitted signal multiply by doppler shift
s2=s;                             %the transmitted signal
c=conv(s1,fliplr(s2)).*dt;        %correlation of s1 & s2
z=[z;(abs(c)).^2];                %matrix of the ambiguity function
end
[l,r]=size(z);
t=[fliplr(-t),t(2:N*Tn)];         %resconstruct time axis
figure(1)
mesh(t,fd,z)                      %mesh plot of the ambiguity function
xlabel('delay (PRI)')
ylabel('frequency (PRF)')
```

```
figure(2)
plot(t,z((nx+1)/2,:))                    %plot of cut along time axis
xlabel('delay (PRI)')
grid
figure(3)
plot(fd',z(:,(r+1)/2))                   %plot of cut along frequency axis
xlabel('frequency (PRF)')
grid
%
*************************************************************************
```

```
**************************************************************************
%filename : prog4.m
%Ambiguity function of the discrete frequency pulse
%update : 18/mar/94
%by : Huang, Jen-chih
%
%
clear                                   %clear all the variables
tau=1;                                  %pulse width
df=1;                                   %frequency step
N=4;                                    %# of discrete frequencies
sn=30;                                  %sample rate in delay axis
ny=101;                                 %# of sample in frequency axis
t=[0;N*sn-1]*tau/(N*sn);                % time delay axis
dt=t(2)-t(1);                           %time step
s=[];
m=[1,2,3,4];                           %discrete frequency sequence
for n=1:N
s=[s,exp(j*2*pi*(m(n)-1)*df*t(sn*(n-1)+1:sn*n))];  %envelope of the transmitted signal
end
z=[];
fd=linspace(-4/tau,4/tau,ny);           %frequency axis
for l=1:ny
s1=conj(s).*exp(j*2*pi*fd(l)*t);        %conjugate of s times Doppler shift
s2=s;
c=conv(s1,fliplr(s2)).*dt;              %correlation of s1 & s2
z=[z;(abs(c)).^2];                      %matrix of the ambiguity function
end
t=[fliplr(-t),t(2:N*sn)];               %reconstruct the time delay axis
figure(1)
mesh(t,fd,z)                            %mesh plot of the ambiguity function
title('Ambiguity function of the discrete frequency pulse')
xlabel(' time (pulse width)')
ylabel('frequency (1/pulse-width)')
figure(2)
contour(t,fd,z,40)                      %contour plot of the ambiguity function
title('contour plot of the ambiguity function of the discrete frequency pulse')
xlabel(' time (pulse width)')
ylabel('frequency (1/pulse-width)')
%
**************************************************************************
```

```
**************************************************************************
%filename : proga1.m
%ambiguity function of the single pulse by equation
%update : 20/aug/94
%by : Huang, Jen-chih
%
%
clear;
Ts=1;
nx=101;
tau=linspace(-Ts,Ts,nx);
ny=51;
fd=linspace(-4/Ts,4/Ts,ny);
z=[];
for m=1:ny
f=fd(m);
x=[];
for n=1:nx
 t=tau(n);
 if t>=0
  if f*(Ts-t)==0
    x=[x,(Ts-t)];
  else
    x=[x,(Ts-t).*(sin(pi*f*(Ts-t)))./(pi*f*(Ts-t))];
  end
 else
  if f*(Ts+t)==0
    x=[x,(Ts+t)];
  else
    x=[x,(Ts+t).*(sin(pi*f*(Ts+t)))./(pi*f*(Ts+t))];
  end
 end
end
z=[z;x];
end
z=(abs(z)).^2;
mesh(tau,fd,z)
xlabel('delay (pulse-width)')
ylabel('frequency (1/pulse-width)')
contour(tau,fd,z,40)
**************************************************************************
```

```
**************************************************************************
%filename : proga2.m
%Ambiguity function of the linear frequency modulation pulse by equation
%
clear;
Ts=1;
mu=4;
nx=101;
tau=linspace(-Ts,Ts,nx);
ny=51;
fd=linspace(-4/Ts,4/Ts,ny);
z=[];
for m=1:ny
x=[];
for n=1:nx
 t=tau(n);
 f=fd(m)-mu*t;
 if t>=0
  if f*(Ts-t)==0
    x=[x,(Ts-t)];
  else
    x=[x,(Ts-t).*(sin(pi*f*(Ts-t)))./(pi*f*(Ts-t))];
  end
 else
  if f*(Ts+t)==0
    x=[x,(Ts+t)];
  else
    x=[x,(Ts+t).*(sin(pi*f*(Ts+t)))./(pi*f*(Ts+t))];
  end
 end
end
z=[z;x];
end
z=(abs(z)).^2;
mesh(tau,fd,z)
xlabel('delay (pulse-width)')
ylabel('frequency (1/pulse-width)')
contour(tau,fd,z,40)
%
**************************************************************************
```

```
*************************************************************************
%filename : proga3.m
%Ambiguity function of the pulse radar by equation
% update : 20/aug/94
%by : Huang,Jen-chih
clear;
Ts=0.2;
Tr=1;
d=Ts/Tr;
N=4;
nx=161;
tau=linspace(-N*Tr,N*Tr,nx);
ny=61;
fd=linspace(-10,10,ny);
p=floor(tau/Tr);
r=(tau/Tr)-p;
z=[];
for m=1:ny
x=[];
f=fd(m);
for n=1:nx
 t=tau(n);
 pp=p(n);
rr=r(n);
 if rr>=0 & rr<d
  if f==0
    x=[x,(Ts-rr*Tr)*(N-abs(pp))];
  else
     x1=(sin(pi*f*(Ts-rr*Tr)))./(pi*f*(Ts-rr*Tr));
     if rem(f*Tr,1)==0
       x2=N-abs(pp);
     else
       x2=(sin(pi*f*(N-abs(pp))*Tr))./(sin(pi*f*Tr));
     end
    x=[x,(Ts-rr*Tr).*x1*x2];
  end
else
   if f==0
    x=[x,(Ts+(rr-1)*Tr)*(N-abs(pp+1))];
  else
     x1=(sin(pi*f*(Ts+(rr-1)*Tr)))./(pi*f*(Ts+(rr-1)*Tr));
     if rem(f*Tr,1)==0
```

```
      x2=N-abs(pp+1);
    else
      x2=(sin(pi*f*(N-abs(pp+1))*Tr))./(sin(pi*f*Tr));
    end
   x=[x,(Ts+(rr-1)*Tr).*x1*x2];
  end
else
  x=[x,0];
end
end
z=[z;x];
end
z=(abs(z)).^2;
figure(1)
mesh(tau,fd,z)
xlabel('delay (pulse-width)')
ylabel('frequency (1/pulse-width)')
figure(2)
contour(tau,fd,z,40)
%
*************************************************************************
```

```
**************************************************************************
%filename : proga4.m
%Ambiguity function of the stepped frequency radar by equation
% update : 20/aug/94
%by : Huang, Jen-chih
clear;
Ts=0.2;
Tr=1;
df=2;
d=Ts/Tr;
N=4;
nx=161;
tau=linspace(-N*Tr,N*Tr,nx);
ny=61;
fd=linspace(-10,10,ny);
p=floor(tau/Tr);
r=(tau/Tr)-p;
z=[];
for m=1:ny
x=[];
f=fd(m);
for n=1:nx
 t=tau(n);
 pp=p(n);
 rr=r(n);
 f1=f-pp*df;
 f2=f-(2*pp+rr)*df;
 f3=f-(pp+1)*df;
 f4=f-(2*pp+rr+1)*df;
 if rr>=0 & rr<d
  if f1==0
    x1=1;
  else
    x1=(sin(pi*f1*(Ts-rr*Tr)))./(pi*f1*(Ts-rr*Tr));
  end
  if rem(f2*Tr,1)==0
    x2=N-abs(pp);
  else
    x2=(sin(pi*f2*(N-abs(pp))*Tr))./(sin(pi*f2*Tr));
  end
    x=[x,(Ts-rr*Tr).*x1*x2];
elseif rr<1 & rr>=(1-d)
```

```
   if f3==0
     x1=1;
   else
     x1=(sin(pi*f3*(Ts+(rr-1)*Tr))./(pi*f3*(Ts+(rr-1)*Tr));
   end
   if rem(f4*Tr,1)==0
     x2=N-abs(pp+1);
   else
     x2=(sin(pi*f4*(N-abs(pp+1))*Tr))./(sin(pi*f4*Tr));
   end
     x=[x,(Ts+(rr-1)*Tr).*x1*x2];
else
   x=[x,0];
end
end
z=[z;x];
end
z=(abs(z)).^2;
figure(1)
mesh(tau,fd,z)
xlabel('delay (pulse-width)')
ylabel('frequency (1/pulse-width)')
figure(2)
contour(tau,fd,z,40)
%
**************************************************************************
```

```
**************************************************************************
%filename : proga5.m
%Ambiguity function of the discrete frequency modulation pulse by equation
% update : 20/aug/94
%by : Huang, Jen-chih
clear;
N=4;
T=1/N;
df=2;
d=Ts/Tr;
nx=121;
tau=linspace(-N*Tr,N*Tr,nx);
ny=61;
fd=linspace(-4,4,ny);
p=floor(tau/Tr);
r=(tau/Tr)-p;
z=[];
for m=1:ny
x=[];
f=fd(m);
for n=1:nx
 t=tau(n);
 pp=p(n);
 rr=r(n);
 f1=f-pp*df;
 f2=f-(2*pp+rr)*df;
 f3=f-(pp+1)*df;
 f4=f-(2*pp+rr+1)*df;
  if f1*(Ts-rr*Tr)==0
    x1=1;
  else
    x1=(sin(pi*f1*(Ts-rr*Tr)))./(pi*f1*(Ts-rr*Tr));
  end
  if rem(f2*Tr,1)==0
    x2=N-abs(pp);
  else
    x2=(sin(pi*f2*(N-abs(pp))*Tr))./(sin(pi*f2*Tr));
  end
  y1=(Ts-rr*Tr).*exp(j*pi*f1*(Ts+rr*Tr)).*x1.*exp(j*2*pi*pp*df*t)
                          .*exp(j*pi*f2*(N-1+pp)*Tr).*x2;
  if f3*(Ts+(rr-1)*Tr==0
    x3=1;
```

```
  else
    x3=(sin(pi*f3*(Ts+(rr-1)*Tr))./(pi*f3*(Ts+(rr-1)*Tr));
  end
  if rem(f4*Tr,1)==0
    x4=N-abs(pp+1);
  else
    x4=(sin(pi*f4*(N-abs(pp+1))*Tr))./(sin(pi*f4*Tr));
  end
   y2=(Ts+(rr-1)*Tr).*exp(j*pi*f3*(Ts+(rr-1)*Tr)).*x3.*exp(j*2*pi*(pp+1)*df*t)
                        .*exp(j*pi*f4*(N+pp)*Tr).*x4;
    x=[x,y1+y2];
end
z=[z;x];
end
z=(abs(z)).^2;
figure(1)
mesh(tau,fd,z)
xlabel('delay (pulse-width)')
ylabel('frequency (1/pulse-width)')
figure(2)
contour(tau,fd,z,40)
%
**************************************************************************
```

LIST OF REFERENCES

1. Donald R. Wehner, *High Resolution Radar*, Artech House Inc., 1985.

2. James A. Scheer, and James L. Kurtz, *Coherent Radar Performance Estimation*, Artech House Inc., 1993

3. Peyton Z. Peebles, Jr., *Probability, Random Variables, and Random Signal Principles*, Second Edition, McGraw-Hill, Inc., 1987

4. A.I. Sinsky, and C.D. Wang, *Standarization of the Definition of the Radar Ambiguity Function*, IEEE Transsactions on Aerospace and Electronic Systems, Vol. AES-10, pp. 532-533, July 1974

5. Merill I. Skolnik, *Introduction to Radar Systems*, Second Edition, McGraw-Hill, Inc., 1980.

6. David C. Lush, *Airborne Radar Analysis Using the Ambiguity Function*, pp. 600-605, IEEE International Radar Conference, 1990.

7. H.R. Ward, *Doppler Processor Rejection of Range Ambiguous Clutter*, IEEE Transactions on Aerospace and Electronic Systems, Vol. AES-11, no. 4, pp. 519-522, July 1974

INITIAL DISTRIBUTION LIST

1. Defence Technical Information Center — 2
   Cameron Station
   Alexandria VA 22304-6145

2. Library Code 52 — 2
   Naval Postgraduate school
   Monterey Ca 93943-5101

3. Chairman Code EC — 2
   Department of Elecrtical and Computer Engineering
   Naval Postgraduate school
   Monterey Ca 93943-5121

4. Chairman Code 3A — 2
   Undersea Warfare Systems\EW
   Naval Postgraduate school
   Monterey Ca 93943-5124

5. Dr. Gurnam S.Gill, Code EC/Gl — 5
   Department of Electrical and Computer Engineering
   Naval Postgraduate school
   Monterey Ca 93943-5121

6. Dr. Tri T. Ha, Code EC/Ha — 1
   Department of Electrical and Computer Engineering
   Naval Postgraduate school
   Monterey Ca 93943-5121

7. Library
   Chung Shang Institute of Science and Technology — 1
   P.O. Box 90008, Lung-Tan, Tao-Yuan
   33500, Taiwan, R.O.C.

8. Library
   Chung Cheng Institute of Technology — 1
   P.O. Box 90047, Ta-Hsi, Tao-Yuan
   33500, Taiwan, R.O.C.

9. Maj. Huang Jen-Chih 1
P.O. Box 90008-6-14, Lung-Tan, Tao-Yuan
33500, Taiwan, R.O.C.